

NATIONAL ADVISORY COMMITTEE FOR AERONAUTICS

**WAR  
TECHNOLOGY  
INSTITUTE OF TECHNOLOGY**  
**WARTIME REPORT**

ORIGINALLY ISSUED

October 1941 as

Report

THE EFFECTS OF HUB DRAG, SOLIDITY, DUAL  
ROTATION, AND NUMBER OF BLADES UPON THE  
EFFICIENCY OF HIGH-PITCH PROPELLERS

By Elliott G. Reid  
Stanford University

**CASE FILE  
COPY**



WASHINGTON

NACA WARTIME REPORTS are reprints of papers originally issued to provide rapid distribution of advance research results to an authorized group requiring them for the war effort. They were previously held under a security status but are now unclassified. Some of these reports were not technically edited. All have been reproduced without change in order to expedite general distribution.

THE EFFECTS OF HUB DRAG, SOLIDITY, DUAL  
ROTATION, AND NUMBER OF BLADES UPON THE  
EFFICIENCY OF HIGH-PITCH PROPELLERS

By Elliott G. Reid

SUMMARY

This report describes an investigation of the effects of hub drag, solidity, dual rotation, and number of blades upon the efficiency of high-pitch propellers.

Preliminary tests made with six-blade propellers demonstrated that slightly greater efficiencies were obtained with a spinner of 0.12D than with one of 0.28D.

Two-, three-, four-, and six-blade single-rotating propellers, and four- and six-blade dual-rotating propellers, equipped with spinners of the smaller size, were then tested at blade angles of  $35^{\circ}$  to  $65^{\circ}$  at 0.75R. Comparison of the results with those of previous tests made with bare hubs reveal substantial increases of thrust, very small effects upon power, and marked improvements in efficiency. These improvements increase with  $V/nD$  and are greater for single- than for dual-rotation models.

The effects of solidity, dual rotation, and number of blades upon the performance characteristics of constant-speed propellers with spinners are analyzed by a new method. With such propellers, it is found that marked improvements in take off and climbing performance can be obtained by increasing solidity and introducing dual rotation, and that reduction of the number of blades - accompanied by compensating increase of width - has a beneficial, rather than adverse, effect at low speed and a negligible one at high speed.

The general conclusion is drawn that blade loading is a more reliable index of propeller performance than is disk loading.

## INTRODUCTION

Two previous Stanford investigations of tandem (dual rotation) propellers are described in references 1 and 2; the hubs of the models used in these experiments were fully exposed. Other tests of some of the same models (reference 3) have demonstrated that substantial beneficial effects are obtained by enclosing the hubs within small spinners. Full-scale tests (reference 4) substantiate these results and indicate that the influence of hub drag increases with the pitch of the propeller.

Since the apparent superiority of the tandem arrangement over the conventional one also increased with pitch when the hubs were unshielded, it was considered desirable to undertake a broad investigation of the effects of hub drag upon the efficiency of high-pitch propellers of both single- and dual-rotating types. And, as such an investigation would necessarily involve most of the experimental work required for analysis of the effects of solidity, dual rotation, and number of blades upon propulsive efficiency, a slight enlargement of the program enabled the inclusion of these objectives.

Presented in this report are the results of these experiments which were carried out for the NACA in the Guggenheim Aeronautic Laboratory of Stanford University.

## APPARATUS AND METHODS

Wind tunnel and dynamometer. - The 7-1/2 foot Eiffel-type tunnel and the dynamometer used for these tests have been described in reference 1. The dynamometer enables determination of the total thrust and the torque of each member of a tandem combination; its shrouding was slightly modified during the present tests to blend smoothly into the lines of the spinners, which were attached to the model propellers.

Model propellers. - The blades of the models used in these experiments were of NACA type E and have been used in several previous investigations. (See references 1, 2, 3, and 5.) Their general appearance is illustrated by figures 1 to 5; blade-form curves are given in figure 6 and a complete drawing may be found in reference 5. The fact that the shanks of these blades have streamline profiles should be noticed particularly because this feature has such an important bearing upon the question of optimum spinner diameter.

All of the models were 36 inches in diameter. Attention is called to the uniformity of size because previously tested six-blade models have been 37 inches in diameter; this irregularity was eliminated by reconstruction of the six-way hub. In all but two special models (used to investigate the effect of number of blades with fixed solidity) the blade width was that defined by the  $b/D$  curve designated E in figure 6; at corresponding radii, the chords of the wider blades, E' and E'' were, respectively,  $4/3$  and  $3/2$  those of the E blades. All blade-angle values refer to the section at  $0.75R$ .

Spinners. - Spinners of two sizes were tested; their forms are illustrated by figures 1 to 5. The forward sections were halves of ellipsoids of revolution and the rear sections were circular cylinders. The half-ellipsoids had axial lengths equal to their maximum diameters which were 4.25 inches (0.118D) and 10.00 inches (0.278D). The planes of rotation of single propellers and those of the forward members of tandem combinations were located 3.625 inches (0.101D) aft of the bases of the ellipsoidal noses. The concentric dynamometer shrouds slightly overlapped the spinners, cleared them radially by 0.05 inch and terminated 2.2 inches aft of the plane of rotation of the single propellers and 1.4 inches aft of the plane of the rear propeller when two were mounted in tandem.

The small spinners had the minimum diameter which would permit enclosure of the hubs; they were pierced with holes just large enough to admit the circular blade shanks and the butts of the blades touched the spinners when set at large angles. (See fig. 4.) The large spinners enclosed considerable portions of the blades and the diameter of the circular apertures was therefore slightly greater than the blade chord. All of the spinners had internal diaphragms which prevented centrifugal pumping action, that is, drawing air from the base of the spinner and discharging it through the blade apertures. To provide strictly comparable blade-root conditions, the apertures in the large spinners were closed with cellophane tape and when small spinners were used the irregularities at the roots of the blades were filled with plasticine. The terms "plain" and "filleted" blade roots are used to distinguish the conditions illustrated by figures 4 and 5, respectively.

Tests. - To determine the effects of spinner diameter, preliminary tests were made with six-blade model propellers which were fitted successively with the large and small spinners. In the case of the small one, tests were made at blade angles of  $35^\circ$ ,  $45^\circ$ ,  $55^\circ$ , and  $65^\circ$  with plain blade roots and at  $45^\circ$  and  $65^\circ$  with filleted roots.

The blade apertures in the large spinner were closed during tests made with blade angles of 35°, 45°, 55°, and 65° but the effects of opening them were determined for settings of 45° and 65°.

The results of the foregoing tests demonstrated that with comparable conditions at the blade roots, that is, filleted roots with the small spinner and closed blade apertures with the large one, the small spinner was slightly superior at all blade angles. Spinners of C.118D were therefore used to complete the following program of tests:

Arrangement	Blade type	No. of Blades	$\beta$ at 0.75R (deg)
Single rotation	E	6	35, <sup>1</sup> 45, 55, <sup>1</sup> 65
Single rotation	E	<sup>3</sup> 4	35, <sup>1</sup> 45, 55, <sup>1</sup> 65
Dual rotation <sup>2</sup>	E	6	35, <sup>1</sup> 45, 55, <sup>1</sup> 65
Dual rotation <sup>2</sup>	E	4	35, <sup>1</sup> 45, 55, <sup>1</sup> 65
Single rotation	E	<sup>4</sup> 3	35, 45, 55, 65
Single rotation	E'	<sup>3</sup> 3	35, 45, 55, 65
Single rotation	E''	<sup>4</sup> 2	35, 45, 55, 65

<sup>1</sup>Indicates that an additional test was made with filleted blade roots.

<sup>2</sup>Blade angles are those of forward (r.h.) propeller; blade angles of rear (l.h.) propeller were identical with those specified in reference 2, i. e.

$\beta$ (r.h.)	35	45	55	65	deg
$\beta$ (l.h.)	34.3	43.8	53.1	62.5	deg

<sup>3</sup>and <sup>4</sup> identify propellers of equal solidities.

Tests were made in accordance with the usual Stanford laboratory practice of driving model propellers at constant rotative speeds and varying  $V/nD$  by altering the wind speed. The rotative speeds utilized for tests made with blade angles of  $35^\circ$ ,  $45^\circ$ ,  $55^\circ$ , and  $65^\circ$  were approximately 1500, 1100, 865, and 625 rpm, respectively. These values are substantially equal to those used for the same blade settings in the tests covered by references 1, 2, and 3. Two complete tests were made with each model at each blade setting; the velocities used in the second were intentionally staggered with respect to those of the first, and blade angles were checked between tests. This somewhat unconventional technique yielded very gratifying results; it led to the discovery of one error in blade setting, to unusually precise definition of discontinuities (e.g. the break in the  $C_p$  curve for the "E" blades at  $35^\circ$ ), and to the discovery of some hysteresis effects upon the characteristics of dual-rotating propellers when set at  $65^\circ$ .

The only entirely new element of testing procedure adopted for these experiments was the observation and regulation of the pressures on the backs of the spinners. This was relatively unimportant in the case of the small spinner but seriously erroneous thrust readings would have been recorded if no attention had been paid to the pressures built up within the shroud behind the large spinner.

To eliminate such extraneous forces, the combination of bleeder orifices with an adjustable flap ring was first used and this was later supplanted by a variable scoop for adjustment of the pressure inside the shroud. As the variation with  $V/nD$  of the pressures at the several necessary openings in the shroud made it impossible, even with a single model, to maintain equality of the internal and static pressures, the pressure control device was so adjusted as to equalize them at the  $V/nD$  for maximum efficiency and a shroud pressure run was made before each model propeller test. The thrusts observed during the latter were subsequently corrected for deviations of the shroud pressure from the static pressure of the undisturbed stream.

Under these conditions, the spinner thrust corrections were less than 1 percent of the measured thrust except at values of  $V/nD$  well above or below that for maximum efficiency and they exceeded 3 percent only with the large spinner. Moreover, the accuracy with which the shroud pressures were determined enabled calculation of the corrections with an accuracy much greater than that of force observation. Therefore the corrected thrusts may be confidently accepted as those which correspond to the existence of static pressure over the backs of the spinners.

## RESULTS

The observed data have been reduced to the usual coefficient forms

$$C_T = \frac{T}{\rho n^2 D^4} \quad C_P = \frac{P}{\rho n^3 D^5} \quad \eta = \frac{C_T}{C_P} \times \frac{V}{nD} \quad C_S = \frac{V}{nD} \sqrt[5]{\frac{1}{C_P}}$$

Use has also been made of what will be called the "thrust power coefficient"; it is defined as  $C_{PT} = \eta C_P$ . The symbol  $\Delta C_P$  is used to represent the difference between the power coefficient for the forward (r.h.) and rear (l.h.) members of tandem combinations, that is,

$$\Delta C_P = C_P \text{ (r.h.)} - C_P \text{ (l.h.)}$$

and is therefore positive when the forward propeller absorbs more than one-half of the total power input.

The reduced numerical data for all of the tests are presented in tables 1 to 42; an index of tables precedes the first one.

Values from a representative table have been plotted in figure 7 to illustrate the degree of agreement between the results of check tests.

The effects of varying the spinner diameter in the case of the six-blade model are summarized by the curves of figure 8.

The characteristics of seven types of high-pitch propellers - with spinners of  $0.118D$  - are presented in the logarithmic charts (figures 9 to 15). Comparable curves for the same propellers without spinners also appear in these figures. Envelope efficiency curves for all but the wide-blade models are shown in figure 16 and, in figure 17, the envelopes which correspond to small spinners and plain blade roots are superimposed.

Various charts derived from figures 9 to 15 will be referred to in the following discussion. An index of charts follows figure 5.

## DISCUSSION

Comparison of large and small spinners. - Inspection of the curves in figure 8 reveals a rather surprising fact. It is that small irregularities of form at the junctions of propeller blades with a spinner may have greater influence upon the efficiency of that propeller than does doubling the spinner diameter. It therefore appears that a fair appraisal of the relative merits of different spinners can be made only when comparable conditions exist at the blade roots. Moreover, since the detrimental effects of such irregularities increase with blade angle, this discovery has an important bearing on the design of spinners and blade shanks (or cuffs) intended for high-speed aircraft.

The superimposed envelope efficiency curves at the bottom of figure 8 show that when blade-spinner interference effects are minimized, the influence of spinner diameter upon efficiency is relatively slight. The small order of the difference between the efficiencies attained with the large and small spinners will probably be surprising to the advocates of both varieties, but the allowable latitude of design indicated by this result cannot fail to be welcomed.

Although the spinner of minimum diameter was found to be superior in the present instance, which involved blades with streamline shanks, there is good reason to believe that this might not have been the case if the experiments had been made with round-shank blades. The broad question of optimum spinner diameter thus remains unsettled, but these results clearly indicated the desirability of using the smaller spinner throughout the remainder of this investigation.

Effects of spinners. - The effects of adding spinners to model propellers of seven types are illustrated by figures 9 to 15. Before examining these results in detail, it may be worth while to consider the potential sources of spinner effects upon propeller characteristics.

First, and most important, the hub of a propeller, when unshielded, experiences a considerable drag. This neutralizes a part of the thrust actually produced by the blades and thus reduces the effective thrust. Suppression of this drag is the primary object of enclosing the hub with a spinner. The resultant benefits may be augmented, of course, by making the spinner diameter somewhat larger than that of the hub when the blade shanks are of crude form. However, it should be remembered that as spinner diameter increases, the

effects of increased disk loading and axial velocity tend to nullify the benefits of suppressing shank drag. It is interesting to note that, if the drag coefficient of the hub be considered constant for all operating conditions, the effect of reducing this coefficient would be to increase the thrust coefficient by an amount proportional to  $(V/nD)^2$ . Now, since the thrust coefficients at which high-pitch ( $\beta = 35^\circ$  to  $65^\circ$ ) propellers attain their maximum efficiencies do not increase as rapidly as the corresponding values of  $(V/nD)^2$ , the suppression of hub drag may be expected to produce improvements in efficiency which will increase with the pitch.

Another obvious source of influence is the reduction of resistance to rotation effected by enclosing the hub within a body of revolution. An approximate analysis of this effect leads to the anticipation of a small and uniform reduction of the power coefficient over the whole operating range.

The third source of spinner effects is equally apparent but the consequences cannot be so readily estimated; it is the alteration of the distribution of velocity over the propeller disk. However, this appears likely to be of minor importance unless relatively large spinners are used.

The experimentally determined effects will now be viewed against this background. Examination of figures 9 to 15 reveals that the results of the addition of spinners are, in general, to augment the thrust coefficient by a substantial amount, to alter the power coefficient almost negligibly and, therefore, to maintain or improve the efficiency under all operating conditions. The improvements of thrust and efficiency increase with  $V/nD$  - and, therefore, with blade angle - and the changes of power coefficient are seen to be of secondary importance.

Two very significant facts are revealed by the envelope efficiency curves of figure 16. The first is that the efficiency of a dual-rotating propeller is improved less by the addition of a spinner than is that of the single propeller of equal solidity which has the same total number of blades. The second is that the magnitude of the gain in efficiency due to the use of a spinner is very slightly altered as the number of blades is increased from three to six.

For case of comparison, efficiency envelopes for the five models which incorporate E-type blades are presented in figure 17. The most noteworthy characteristic of these curves is their flatness. They strongly resemble the curves predicted by application of the simple blade-element theory of a "representative element." It is interesting to observe that hub drag has obscured this characteristic in previous work done without spinners. It now appears that the use of very high pitch propellers is not necessarily accompanied by a serious loss of efficiency; in fact, it is apparent that high-solidity, dual-rotating propellers may develop efficiencies in excess of 85 percent with blade angles as great as  $65^\circ$ .

It is also shown by figure 16 that the apparent superiority of the dual-rotation arrangement over the conventional one is considerably less when spinners are used than was indicated by the results of earlier tests made with bare hubs. However, it cannot be too strongly emphasized that mere comparison of the envelope efficiency curves is an entirely inadequate basis for appraisal of the merits of different propellers and that this is particularly true under the condition of constant-speed operation. A more comprehensive method of analysis is outlined in the following section and further reference will be made to the question of single versus tandem propellers.

Comparison of constant-speed propellers. - Although a contrary view is somewhat widely held, the advent of constant-speed propellers has greatly simplified the problem of selecting the optimum design for a given set of operating conditions.

In the case of the fixed- or controllable-pitch propeller, neither the Eiffel logarithmic chart nor the more frequently used "design chart" ( $\eta$  and  $V/nD$  vs.  $C_g$ ) yields the desired results which, in the final analysis, are simply curves of available thrust horsepower versus velocity ( $thp_a$  vs.  $V$ ) for each of the designs under consideration. For any thorough comparison, these curves should extend over the entire range of operating speed. Unfortunately, the afore-mentioned charts enable direct comparisons to be made under only one operating condition, that is, top speed or climb. As is clearly explained in chapter X of reference 6, the only completely satisfactory procedure is to compute, plot, and compare curves of  $thp_a$  versus  $V$  for several alternative designs. The necessity for this laborious procedure arises largely from the wide divergence in the character of the variations of power (or torque) with rotative speed among modern aircraft engines. On the other hand, the use of a constant-speed propeller enables the operation of any aircraft engine

at constant values of power and rpm at all flight speeds. The previous complication is thus completely excluded and a new and much simpler method of comparison is made possible.

A relatively new type of chart is particularly useful for this purpose. Originally developed for use in a graphical method of performance prediction (reference 7), it enables direct comparison, under the conditions of constant speed operation, of curves of  $thp_a$ ,  $\eta$  or  $\eta C_p$  versus  $V$  or  $V/nD$  for any range of flight speed. The multiple identity of the curves and the simplicity of their preparation are explained below.

To understand the development of the chart, one has but to recognize the fact that when a constant-speed propeller is operated at fixed values of power input, rotative speed, and air density, the variation of blade angle with air speed is exactly that required to maintain the power coefficient ( $C_p = 550 \text{ bhp}/\rho n^3 D^5$ ) at a constant value. Under these conditions

$$thp = \eta \text{ bhp} = \eta C_p (\rho n^3 D^5 / 550) = \eta C_p (\text{constant})$$

This means, simply, that the ordinates of the curve of  $thp_a$  versus  $V$  which corresponds to a particular value of  $C_p$  are directly proportional to the values of  $\eta$  which are realized when the blade angle is automatically adjusted so that the same amount of power is absorbed at all air speeds without variation of the rpm.

Such curves of  $\eta$  versus  $V/nD$  can be easily constructed when contours of  $\eta$  are superimposed upon a logarithmic chart of  $C_p$  versus  $V/nD$  for a given type of propeller with its blades set at various angles. An example is shown in figure 18 where the construction of the curve of  $\eta$  versus  $V/nD$  for  $C_p = 0.4$  is illustrated. It will be noted that proper location of scales enables the same curve to define both  $\eta$  and  $C_{PT}$  ( $C_{PT} = \eta C_p$ ).

The use of logarithmic scales also permits interpretation of the curves of  $C_{PT}$  versus  $V/nD$  as curves of  $thp_a$  versus  $V$ ; this is the distinctive characteristic of the original Eiffel logarithmic propeller chart.<sup>1</sup> Thus the construction of a family of such curves for each type of propeller effectively enables direct comparison of the curves of  $thp_a$  versus  $V$  for all types under all conditions of constant-speed operation.

---

<sup>1</sup>Scales for  $P$  and  $V$  may be correlated with those for  $C_p$  and  $V/nD$ , respectively, by use of equations (1) and (2) of reference 7.

Characteristics of constant-speed propellers. - Curves of the kind just described have been prepared for all of the propellers tested during the present investigation; they appear in figures 19 to 25. These families have certain common characteristics which merit special attention. Most important, perhaps, is the definition of an envelope by each family and the convergence of the curves for small values of  $C_p$  as  $V/nD$  decreases. This convergence and the existence of an envelope reveal the fact that, quite aside from compressibility losses, the thrust produced by a constant-speed propeller at relatively low forward speeds and constant rpm does not increase continuously with power input. On the contrary, with continuous increase of power at fixed forward and rotative speeds, the thrust (which is proportional to  $C_{PT}$ ) first increases, then levels off, and finally declines very rapidly. Thus, optimum thrust may be attained at part throttle under certain low speed conditions.

The secondary noteworthy feature is the uniformity of slope of the left-hand portions of the majority of the  $C_{PT}$  curves (approximately  $45^\circ$ ). The significance of this feature is revealed by replotting one of the families of curves to Cartesian coordinates; figure 26 is such a replot of figure 20. The  $45^\circ$  lines of the logarithmic chart are transformed into straight lines which radiate from the origin. This rectilinear characteristic indicates that the thrust of a constant-speed propeller is practically constant throughout the take-off run.

A third feature of importance is also apparent in figure 26; it is the very flat top which characterizes the  $C_{PT}$  (or  $\eta$ ) versus  $V/nD$  curves for constant-speed propellers. The rate at which the efficiency declines beyond the peak is so unlike that for the fixed-pitch propeller as to completely revise previous ideas of the sacrifice of top speed enforced by the use of a propeller which attains peak efficiency at an air speed well below the maximum. This characteristic difference may be clearly visualized by comparing the  $\eta$  (or  $C_{PT}$ ) versus  $V/nD$  curve for  $C_p = 0.4$  in figure 18 with the efficiency curve for  $\beta = 45^\circ$  in figure 10; both refer to the four-blade single-rotating propeller and peak at approximately equal values of  $V/nD$ .

Envelope curves of  $C_{PT}$  versus  $V/nD$  for propellers of five types are shown in figure 27. Their practical significance will become apparent with further discussion.

Effects of solidity and dual rotation. - The effects of solidity and of dual rotation upon the performance characteristics of constant-speed propellers are illustrated by figures 30 to 32. In comparing these curves of  $C_{PT}$  (or  $\eta$ ) versus  $V/nD$ , it should be kept in mind that each group is equivalent to a set of curves of  $thp_a$  versus  $V$  for propellers of five different types, all of the same diameter and all operating under identical conditions of air density, rotative speed, and brake-horse-power input. Although the values of  $C_p$  which have been chosen for comparison (0.3 to 0.6) may seem unfamiliarly large, it is emphasized that even this range does not actually include the upper limit of current design practice. Figures 28 and 29 will help to clarify this point.

Figure 28 shows  $C_p$  to be a function of  $hp/D^2$ ,  $V_T$  (the tangential tip speed) and air density, or altitude. The relationship between these quantities is implicitly expressed by the definitive equation

$$C_p = 550 \text{ bhp}/\rho n^3 D^5$$

The explicit form is obtained when the product  $nD$  is replaced by  $V_T/\pi$  and  $\rho_0$  is substituted for  $\rho$ , that is,

$$C_p = \frac{\text{bhp}}{D^2} \frac{1}{V_T^3} \frac{1}{\sigma} \left[ \frac{550 \pi^3}{\rho_0} \right]$$

The oblique lines of the chart define the sea-level values of  $C_p$ ; values for other altitudes are obtained by adding to the ordinates of the sea-level lines the increments shown on the altitude scale. The values of allowable tangential tip speed can be read directly from figure 29 for any combination of air speed and allowable resultant tip speed ( $V_R$ ).

Values of  $hp/D^2$  currently range from 1.0, for 50-horsepower units, up to 10 or 11 for engines of the 2000-horsepower class. In the case of a modern fighter, if  $V_R$  is limited to 900 feet per second,  $V_T$  cannot exceed about 690 feet per second when  $V = 400$  miles per hour. With  $V_T = 690$  feet per second and  $hp/D^2 = 10$  at 25,000 feet (attainable with turbosupercharging),  $C_p$  is found to be just about 0.5. This must not be thought an extreme case for, in designs now under construction,  $C_p$  is expected to exceed 0.6 at altitude and to approach 0.25 in take-off at sea level. Thus the curves of figures 30 to 32 correspond closely to the conditions of modern military (and probably future civil) design.

Preliminary examination of these curves reveals that the maximum values of  $C_{PT}$  and  $\eta$  (or  $thp_a$ ) differ relatively little. The most striking effect of increasing the solidity of a constant-speed propeller is seen to be the flattening of the peak and leftward displacement of the curve of  $\eta$  versus  $V/nD$ . It will also be noticed that, whereas the value of  $V/nD$  for  $\eta_{max}$  decreases as the solidity is increased, the curves for single- and dual-rotating propellers of equal solidity peak at approximately equal values of  $V/nD$ . And finally, it appears that the introduction of dual rotation without change of solidity has a minor effect upon  $\eta_{max}$  but a major one upon the value of  $\eta$  throughout the range of  $V/nD$  below the peak.

Before discussing these phenomena in detail, it would appear that two questions should be clarified. The first is: Are the effects described above substantiated by full-scale test data or are they, perhaps, simply exaggerated manifestations of scale effect at low Reynolds numbers? The second is: If these phenomena cannot be ascribed to scale effect how can such great variations of efficiency at fixed values of  $C_p$  and  $V/nD$  be correlated with the momentum theory of propulsion which, after all, has furnished fairly reliable indications of the effects of design variations up to the present, but which fails to give any clue to the cause of the solidity effects illustrated by figures 30 to 32?

The answer to the first question is found in reference 8; comparable curves prepared from data contained in that paper are presented in figure 33. While these full-scale results do not agree quantitatively with those of the model tests, the qualitative relationships are so strikingly similar as to preclude any reasonable doubt of the reality of the phenomena. Moreover, it seems probable that much of the quantitative discrepancy may be logically ascribed to differences between the forms of the shanks of the model and full-scale blades; the former were streamlined whereas the latter had circular profiles.

While the benefits derived from dual rotation may be attributed to the reduction of rotational energy losses, the second question must still be answered with respect to the effects of solidity. In each of the figures 30 to 33 it is apparent that there is wide divergence between the efficiencies developed by propellers of various solidities when operating at fixed values of  $C_p$  and  $V/nD$ . This is quite contradictory to the momentum theory which predicts that when  $C_p$  is constant,  $\eta$  will depend only upon  $V/nD$ . The

theoretical relationship is illustrated by the curves designated "ideal efficiency," or  $\eta_1$ , in figures 30 to 33; it is derived from the usual definition of "momentum theory efficiency"

$$\frac{\eta^2}{1-\eta} = \frac{2\rho AV^2}{T}$$

by the substitution of  $\eta P/V$  for  $T$ ,  $\pi D^2/4$  for  $A$ , and  $C_p$  for  $\frac{P}{\rho n^3 D^5}$  and can be reduced to the following form

$$\frac{V}{nD} = \eta \left[ \frac{2C_p}{\pi(1-\eta)} \right]^{1/3}$$

It is now apparent that "disk power loading" is a very unreliable index of propeller efficiency.

The dependence of efficiency upon blade, rather than disk, loading is predicted, however, by both simple blade element and vortex theories. To test this prediction, the curves of figure 34 have been prepared; they illustrate the variations of  $\eta$  with  $V/nD$  for the several types of propeller under conditions of equal blade loading, that is,  $C_p/B = 0.1$  ( $B$  = number of blades). It is immediately apparent that the discrepancies between the curves for single-rotating propellers have been greatly diminished. Even better correlation is obtained when curves of  $\eta/\eta_1$  are plotted in figure 35. Efficiency is thus shown to be unmistakably controlled by blade loading even though the limiting, or ideal, value is fixed by disk loading.

In the light of the foregoing conclusion, the effects of solidity upon the performance characteristics of constant-speed propellers are readily explainable. When the values of  $C_p$  and  $V/nD$  are fixed, the effect of adding more blades is simply to enforce a reduction of the blade loading. Since this can be done only by reducing the angles of attack of the elements and, therefore, the blade angles, an increase of solidity is necessarily accompanied by a reduction of pitch. The relatively low-pitch propeller of great solidity therefore attains its maximum efficiency at a smaller value of  $V/nD$  than does the higher-pitch type of lesser solidity - just as is the case with fixed-pitch propellers. The improvement of efficiency with increasing solidity at small values of  $V/nD$  is similarly explainable: Since the angles of attack under this condition are far greater than that for maximum  $L/D$ , the propeller whose elements have the smallest angles of attack will develop the greatest values of  $T/F$  ( $F$  = elementary tangential force) and, since  $V/nD$  is fixed, will attain the highest value of  $\eta$ .

Figures 30 to 32 show very clearly that, within the range of these tests, the effect of solidity upon the maximum efficiency of a constant-speed propeller is relatively small. However, it is worth noting that when  $C_p = 0.3$ , the three-blade propeller enjoys an advantage of about 3 percent when compared with the six-blade type, but that when  $C_p = 0.6$ , the order of merit is reversed and the values of maximum efficiency differ by 2 percent. The cause of this inversion is readily traced back to the envelopes of efficiency versus  $V/nD$  (fig. 17). Since the effect of increasing solidity is to reduce the value of  $V/nD$  for  $\eta_{max}$ , the three-blade propeller develops maximum efficiencies at values of  $V/nD$  which, when  $C_p = 0.3$  to  $0.6$ , correspond to the declining (right-hand) portion of the envelope. As the number of blades is increased to four and then to six, the corresponding range of  $V/nD$  for  $\eta_{max}$  moves progressively toward the left, that is, toward the region in which the envelope curves are substantially horizontal. Thus the maximum efficiency of the three-blade constant-speed propeller decreases steadily as  $C_p$  increases from  $0.3$  to  $0.6$ , that of the four-blade type diminishes less rapidly and in the case of six blades the variation is practically negligible.

In previous comparisons of single- and dual-rotating propellers, attention has been focused upon the envelope efficiency curves because, when no spinners were used, these curves diverged so remarkably as the pitch became large. The beneficial effect of dual rotation upon the thrust at fixed values of  $C_p$  and  $V/nD$  has been evident in the results of two previous Stanford investigations (reference 1 and 2) but this has not been specifically distinguished from the general improvement of efficiency which was characterized by the marked elevation of the envelope. The first tests of the tandem arrangement made with spinners (reference 8) involved full-scale blades with round shanks and the results indicated that the advantages of dual rotation were very slight as regards peak efficiency; however, attention was called to the augmentation of thrust at reduced values of  $V/nD$ . The form of presentation of the results of the present experiments makes it convenient to examine the efficiency of dual-rotating propellers throughout the useful range of  $V/nD$  under conditions of constant-speed operation and this will be done for obvious reasons.

The net effect of substituting dual rotation for single rotation is clearly apparent in figures 30 to 32; within the range of  $C_p$  covered by these curves, it is a general improvement of efficiency which is relatively small at the peak but much greater at reduced values of  $V/nD$ . It will also be noticed that the magnitude of the improvement increases with both solidity and power coefficient.

The source of this improvement is, of course, indicated in a general way by momentum theory. Since thrust is produced only by the creation of axial momentum, the conversion of rotational momentum into axial momentum results in a corresponding increase of the thrust obtained with a given power input. However, more detailed information can be obtained from figures 9 to 12. By comparing the curves which correspond to single- and dual-rotating propellers of equal solidity, it will be found that at equal blade angles both the power and the thrust are augmented by the use of dual rotation.

The reasons for these increases of thrust and power are not difficult to find. At a given value of  $V/nD$ , the axial velocity through the six-blade dual-rotating propeller will be substantially equal to that for the six-blade single-rotating type because their thrusts are nearly equal. (It may be noted that the slow contraction of the slipstream precludes much change of axial velocity between front and rear members of the tandem combination.) However, the induced tangential velocity in the plane of the forward member of the pair will be little more than one-half as great as the corresponding quantity for the six-blade single-rotating model because their torques have approximately that ratio. Therefore the angles of attack of the elements of the former exceed those of the latter and the thrust and power per blade are correspondingly increased. In the case of the rear member of the tandem pair, the torque is known to be substantially equal to that of the forward one. And because the resultant velocities of corresponding members of the two have practically equal magnitudes, the equality of torque implies approximate equality of the effective angles of attack. This is possible, despite the inequality of blade angles, because the tangential velocity produced by the action of the forward member must largely nullify the self-induced tangential velocity in the plane of the rear one and, for the reasons given in the following paragraph, the result is that the latter's thrust is even greater than that of the forward member. Thus the torques and thrusts of both members of the tandem pair exceed half of the corresponding quantities for the comparable single-rotating type.

The increase of efficiency with fixed values of  $C_p$  and  $V/nD$  is also readily explainable within the range of unstalled operation. For this purpose it will be convenient to replace the forces on a blade of the forward member of a tandem pair by those which act upon a "representative element" and to do the same for one blade of a comparable single-rotating propeller. In considering these forces it must be remembered that, in two-dimensional motion, the relative force vectors for a conventional airfoil maintain a substantially fixed inclination with respect to the relative wind direction throughout the useful range

of  $C_L$ . (See reference 9.) Now, since the introduction of dual rotation causes a reduction of the induced angle of attack which corresponds to a given blade power loading, the inclination of the relative wind with respect to the plane of rotation and that of the resultant force vector to the axial direction, must be correspondingly reduced. The result of the rotation of the force vector is, of course, to augment the ratio  $T/F$  and, therefore, to improve the efficiency. The same explanation holds for the rear member of the tandem pair and the improvement in this case is further augmented by the influence of the forward propeller.

Under the conditions of stalled operation, the direction of the resultant force on a representative element is practically that of a perpendicular to the chord, that is, when the wind direction is fixed, the vector rotates with the profile. (See reference 10.) The superposition of this effect upon the one described in the preceding paragraph causes the improvement of efficiency due to the tandem arrangement to be augmented as  $V/nD$  is reduced.

Further evidence tending to substantiate the hypothesis that induced tangential velocity is the principal factor which controls the efficiency of high-pitch propellers is found in the fact that the power absorbed by the forward member of the six-blade dual-rotating combination is substantially equal to that of the isolated three-blade propeller when both have the same blade angle and operate at the same value of  $V/nD$ . This relationship is not superficially apparent since the values of  $C_p$  for the six-blade dual-rotating type are more than twice those for the three-blade propeller at all but the highest value of  $V/nD$ . However, the power coefficients for the forward and rearward members of the tandem pair are not equal at reduced values of  $V/nD$  and, when values of  $C_p$  (r.h.) are calculated from the tabular data and compared with those for the isolated three-blade propeller, it is found that the differences are negligible until  $V/nD$  becomes relatively small. Then the power absorbed by the three-blade propeller becomes distinguishably larger than that for the forward member of the dual-rotating combination. This apparently indicates that the difference between the axial velocities in these two cases has a practically negligible effect at all but small values of  $V/nD$ . It also furnishes convincing evidence of the validity of one of the fundamental concepts of the vortex theory of propellers, that is, that no upstream rotational flow is induced by a propeller.

Before concluding this discussion of solidity and dual rotation, further attention should be given to the envelope curves of figure 27. These curves simply show the severe limitations which low solidity and

single rotation impose upon the conversion of power into thrust. Their implications with reference to the take-off characteristics of heavily loaded, high-speed aircraft can hardly be overemphasized.

Effect of number of blades. - The characteristics of propellers having three and four blades of NACA type E have been presented in figures 13 and 10, respectively; similar curves for comparable propellers which have fewer and wider blades are shown in figures 15 and 14. The two-blade E" and the three-blade E models have the same solidity; the three-blade E' and four-blade E models are also of equal (but one-third greater) solidity. The characteristics of these same models, without spinners and at blade angles of  $15^\circ$  to  $45^\circ$ , have been previously reported in reference 3.

The characteristics of each pair of comparable models differ so slightly that the effects of altering the number of blades while retaining a given solidity can only be discerned by superposing the curves. To avoid confusion, a single example of such superposition is presented in figure 36. There it is apparent that at equal blade angles the model with the larger number of blades absorbs the greater power and develops the greater thrust at large values of  $V/nD$ ; whereas the reverse is true when  $V/nD$  is small. It also appears that the model with the larger number of blades attains a slightly superior maximum efficiency but that its efficiency is definitely inferior at reduced values of  $V/nD$ . Similar differences characterize comparable curves for both solidities and for all blade angles between  $35^\circ$  and  $65^\circ$ ; the magnitudes of these differences increase somewhat with blade angle and are greater in the case of two versus three blades (small solidity) than those found when three blades are compared with four (large solidity).

Three sets of  $C_{pm}$  (and  $\eta$ ) versus  $V/nD$  curves have been prepared to illustrate the effects of altering the number of blades under various conditions of constant speed operation; they appear in figures 37 to 39. Inspection reveals that maximum efficiency is almost imperceptibly affected but that improved efficiency is obtained at reduced values of  $V/nD$  by reducing the number and increasing the width of the blades.

In seeking an explanation for this somewhat surprising result, it is worth remembering that the elementary vortex theory predicts no change of efficiency with number of blades so long as solidity remains unaltered. To be sure, the necessity for small "tip-loss corrections," which depend upon the number of blades, is recognized, but the analyses of Prandtl and Goldstein (reference 11) indicate that efficiency will

improve as the number of blades increases and that the magnitude of the improvement may be expected to increase with  $V/nD$ . The present results appear to refute both of these predictions.

It appears to the writer that the observed effects of altering the number of blades upon the thrust and power in unstalled operation at a fixed-blade setting are in accordance with certain basic concepts of vortex theory. The primitive form of the so-called vortex theory of propellers assumes an infinite number of blades and relates the induced-velocity components to the total thrust and torque. In reality, however, the induced velocities are controlled by the actual vortices in the wake and their values at points of a given blade will obviously be more influenced by the vortex sheet of that blade than by those of the other blades. Therefore, if the strength of the vortices in the wake of a given blade be increased - as is the case when the blade is widened - the induced velocities at the points of that blade are necessarily correspondingly augmented. Now, since the induced velocities reduce the effective angle of attack when the thrust is positive, it would seem to follow logically that increasing the width of a blade of given pitch angle must reduce the thrust and power coefficients so long as the blade elements remain unstalled.

The reversal of the sense of the thrust and power differences at reduced values of  $V/nD$  (with fixed pitch) is probably the result of a smaller portion of the wide blade being stalled than is the case with the narrow one. It appears that this condition must prevail if the induced angles of attack increase with blade width. If stalled flow extends farther out on the narrow blades than on the wide ones, the forces acting upon the wide-blade propeller will, naturally, be greater.

When the blade angles are fixed, the improvement of efficiency obtained at small values of  $V/nD$  by reducing the number of blades would follow logically if the radial extent of stalled flow were thereby minimized because the ratio  $T/F$  for an element is drastically reduced by the separation of flow. Upon this basis, an even greater increase of efficiency might be expected to occur at a given low value of  $V/nD$  under constant-speed operating conditions because equalization of the values of  $C_p$  for the two models could be accomplished only by making the pitch angles of the narrow blades greater than those of the wide ones.

Thus, acceptance of the concept that induced angles of attack increase with blade width appears to provide the basis for a satisfactory explanation of the principal effects of altering the number of blades in a propeller of given solidity.

Peculiarities of four-blade propellers. - The envelope efficiency curves of figure 17 indicate that four-blade propellers of both single- and dual-rotating types experience greater losses of maximum efficiency with increasing pitch than do the corresponding six-blade models. This characteristic might be ascribed to a more pronounced nonuniformity of disk loading if it were not for the fact that the envelope for the three-blade single-rotating propeller is flatter than that for the comparable four-blade one. When it is noted that the introduction of dual rotation augments the maximum efficiency of both four- and six-blade propellers by amounts which are approximately tripled as  $V/nD$  increases from 2 to 4, one might suspect that the apparent peculiarity had its root in the development of inconsistently high efficiencies by either the three- or both six-blade models. However, this suspicion seems to be unwarranted because the envelopes for the three- and six-blade single-rotation models are, as might be expected, fairly uniformly separated throughout their lengths.

The cause of this apparent inconsistency must therefore be left to conjecture - for the present, at least - but recent reports of unusual vibration in four-blade propellers and the hypothesis that its cause may be traced to the geometry of the vortex system may warrant further investigation of the peculiarities pointed out here.

#### CONCLUDING REMARKS

The results of this investigation indicate that:

(1) Spinner diameter is not critical when the propeller blades have faired shanks, but small irregularities of form at the blade-spinner junctions may have serious adverse effects.

(2) The benefits derived from the use of spinners increase with pitch and are greater for single- than for dual-rotating propellers.

(3) The efficiency versus  $V/nD$  curves for constant-speed propellers have much flatter peaks than those for the fixed-pitch type; they are practically rectilinear throughout the low-speed range and the curves which correspond to various power coefficients define, for each type of propeller, a highly significant envelope.

(4) Increasing solidity by increasing the number of blades will enable take-off and climbing performance to be greatly improved without serious loss of high speed.

(5) Under present design conditions, tandem propellers are only slightly superior to conventional ones of equal solidity as regards high-speed performance but they offer marked advantages in take-off and climb. Their superiority under all conditions will increase as larger values of  $hp/D^2$  are used.

(6) Reducing the number of blades in a constant-speed propeller of given solidity has a negligible effect upon the maximum efficiency but a beneficial one upon low-speed efficiency.

(7) Blade power loading ( $C_p/\text{no. of blades}$ ) is a far better index of propeller efficiency than is disk power loading,  $C_p$ .

In view of these findings, it is suggested that propellers of high solidity offer most of the advantages heretofore obtained by increasing diameter, and their use is recommended for the improvement of take-off and climb. It is pointed out that they promise economies of weight and landing-gear height and that they are particularly suitable for use with two-speed drives. Attention is also called to the now clearly established superiority of the tandem, or dual-rotation, arrangement. Under conditions of constant-speed operation, this is so much greater than that indicated by ordinary envelope efficiency curves that early incorporation of such propellers in high-powered, high-speed airplanes would seem imperative.

Stanford University,  
Stanford University, Calif.

## REFERENCES

1. Lesley, E. P.: Tandem Air Propellers. T.N. No. 689, NACA, 1939.
2. Lesley, E. P.: Tandem Air Propellers - II. T.N. No. 622, NACA, 1941.
3. Lesley, E. P.: Propeller Tests to Determine the Effect of Number of Blades at Two Typical Solidities. T.N. No. 698, NACA, 1939.
4. Biermann, David, and Hartman, Edwin P.: Tests of Five Full-Scale Propellers in the Presence of a Radial and a Liquid-Cooled Engine Nacelle, Including Tests of Two Spinners. Rep. No. 642, NACA, 1938.
5. Lesley, E. P., and Reid, Elliott G.: Tests of Five Metal Model Propellers with Various Pitch Distributions in a Free Wind Stream and in Combination with a Model VE-7 Fuselage. Rep. No. 326, NACA, 1929.
6. Weick, Fred E.: Aircraft Propeller Design. McGraw-Hill Book Co., Inc., 1930.
7. Reid, Elliott G.: Rigorous Performance Prediction Without Drudgery. Jour. R.A.S., vol. XLIV, no. 350, Feb. 1940, pp. 176-194.
8. Biermann, David, and Hartman, Edwin P.: Full-Scale Tests of 4- and 6-Blade Single- and Dual-Rotating Propellers. NACA, ACR, Aug. 1940.
9. Reid, Elliott G.: A Simplified Analysis of Static Longitudinal Stability. Jour. Aero. Sci., vol. 4, no. 9, July 1937, pp. 375-383.
10. Knight, Montgomery: Wind Tunnel Tests on Autorotation and the "Flat Spin." Rep. No. 273, NACA, 1927.
11. Glauert, H.: Aerodynamic Theory, W. F. Durand, ed., vol. IV, pp. 261-269. Julius Springer, Berlin, 1935.

---

 ( ) - Number of blades

S - Single rotation

a - Small spinner

D - Dual rotation

b - Large spinner

---

 Fig. 6. Blade form curves.

7. Typical test results.

8.  $\eta$  vs.  $C_S$  - (6)S, a and b.9.  $C_P$ ,  $C_T$  and  $\eta$  vs.  $V/nD$  - (6)Sa

10. " " " " " - (4)Sa

11. " " " " " - (6)Da

12. " " " " " - (4)Da

13. " " " " " - (3)Sa

14. " " " " " - (3)Sa (E' blades)

15. " " " " " - (2)Sa (E'' blades)

16.  $\eta$  vs.  $V/nD$  - E blade propellers with and without spinners.

17. Envelope efficiency curves - from figure 16.

18. Construction of  $\eta$  vs.  $V/nD$  curve - constant speed propeller.19.  $C_{PT}$  vs.  $V/nD$  - (6)Sa

20. " " " - (4)Sa

21. " " " - (6)Da

22. " " " - (4)Da

23. " " " - (3)Sa

24. " " " - (3)Sa (E' blades)

25. " " " - (2)Sa (E'' blades)

26. Figure 20 transposed to Cartesian coordinates.

27. Envelopes of  $C_{PT}$  vs.  $V/nD$  corresponding to figures 19-23.28. Chart for evaluation of  $C_P$ .

29. Chart for evaluation of allowable tip speed.

30.  $C_{PT}$  and  $\eta$  vs.  $V/nD$  for E-blade models,  $C_P = 0.3$ .31. " " " " " " " " "  $C_P = 0.4$ .32. " " " " " " " " "  $C_P = 0.6$ 33. " " " " " " " " " full scale propellers,  $C_P = 0.4$ .34.  $C_{PT}/B$  and  $\eta$  vs.  $V/nD$  for E-blade models,  $C_P/B = 0.1$ 35.  $\eta/\eta_1$  " " " " " " " " "36.  $C_P$ ,  $C_T$  and  $\eta$  vs.  $V/nD$  - (3)Sa and (2)Sa (E'' blades).37.  $C_{PT}$  and  $\eta$  vs.  $V/nD$  for wide-blade models,  $C_P = 0.3$ .38. " " " " " " " " "  $C_P = 0.4$ 39. " " " " " " " " "  $C_P = 0.6$ .

NACA

Index, Table 1

## INDEX OF TABLES

Table number	Rotation	Blades no. type	Blade angle	Spinner	Root condition	Test number
1	Single	6	35	Small	Plain	1,2
2	"	"	45	"	"	4,5
3	"	"	55	"	"	6,7
4	"	"	65	"	"	8,9
5	"	"	45	"	Paired	12
6	"	"	65	"	"	11B
7	"	"	35	Large	Ap. closed	20,21
8	"	"	45	"	"	13,14
9	"	"	55	"	"	18,19
10	"	"	65	"	"	15,16
11	"	"	45	"	open	22
12	"	"	65	"	"	17
13	"	"	35	Small	Plain	30
14	"	"	45	"	"	26,27
15	"	"	55	"	"	31,32
16	"	"	65	"	"	33,34
17	"	"	45	"	Paired	28
18	"	"	65	"	"	35
19	"	"	35	"	Plain	48,49
20	"	"	45	"	"	50,51
21	"	"	55	"	"	53,54
22	"	"	65	"	"	60,61
23	"	"	45	"	Paired	52
24	"	"	65	"	"	62
25	"	"	35	"	Plain	41,59
26	"	"	45	"	"	38,39
27	"	"	55	"	"	44
28	"	"	65	"	"	47,63
29	"	"	45	"	Paired	40
30	"	"	65	"	"	45
31	"	"	35	"	Plain	66
32	"	"	45	"	"	68
33	"	"	55	"	"	70
34	"	"	65	"	"	73
35	"	"	35	"	"	74
36	"	"	45	"	"	75
37	"	"	55	"	"	76
38	"	"	65	"	"	77
39	"	"	35	"	"	67
40	"	"	45	"	"	69
41	"	"	55	"	"	71
42	"	"	65	"	"	72

TABLE NO. 1

Six-Blade Propeller  
 $\beta = 35^\circ$ Small Spinner  
Plain Blade Roots

Test No. 1					Test No. 2				
V/nD	C <sub>T</sub>	C <sub>P</sub>	$\eta$	C <sub>S</sub>	V/nD	C <sub>T</sub>	C <sub>P</sub>	$\eta$	C <sub>S</sub>
1.648	0.0181	0.0955	0.314	2.636	1.648	0.0237	0.0914	0.428	2.662
1.589	.0530	.1290	.654	2.396	1.583	.0590	.1369	.682	2.359
1.514	.0815	.1635	.755	2.176	1.509	.0832	.1669	.752	2.160
1.436	.1091	.1942	.807	1.993	1.444	.1082	.1942	.804	2.010
1.380	.1275	.2150	.819	1.876	1.374	.1297	.2177	.818	1.865
1.307	.1508	.2379	.829	1.742	1.297	.1518	.2389	.824	1.726
1.241	.1693	.2560	.820	1.628	1.234	.1711	.2587	.817	1.618
1.167	.1899	.2727	.812	1.515	1.162	.1915	.2766	.804	1.504
1.088	.2092	.2887	.789	1.395	1.092	.2082	.2880	.790	1.401
1.021	.2252	.2986	.770	1.312	1.020	.2273	.3003	.772	1.298
.955	.2390	.3095	.738	1.210	.959	.2374	.3077	.740	1.216
.894	.2422	.3188	.679	1.126	.889	.2419	.3198	.673	1.118
.816	.2440	.3213	.620	1.026	.819	.2437	.3208	.622	1.029
.760	.2442	.3226	.575	.954	.757	.2444	.3219	.574	.950
.689	.2461	.3244	.523	.864	.688	.2461	.3249	.521	.861
.618	.2501	.3295	.469	.773	.620	.2493	.3290	.470	.776
.551	.2539	.3339	.418	.687	.552	.2536	.3343	.419	.688
.487	.2558	.3372	.369	.606	.484	.2566	.3372	.368	.554
.402	.2588	.3411	.305	.499	.414	.2576	.3408	.313	.473

TABLE NO. 2

Six-Blade Propeller  
 $\beta = 45^\circ$

Small Spinner  
Plain Blade Roots

Test No. 4						
V/ND	C <sub>T</sub>	C <sub>P</sub>	$\eta$	C <sub>S</sub>	$\eta$	C <sub>S</sub>
2.333	0.0458	0.1960	0.545	3.230	0.596	3.160
2.225	0.0916	0.2753	0.743	2.882	0.708	2.957
2.155	0.1195	0.2985	0.809	2.747	0.785	2.721
2.046	0.1453	0.3225	0.832	2.520	0.816	2.535
1.946	0.1666	0.3504	0.844	2.352	0.838	2.350
1.877	0.1891	0.3802	0.844	2.138	0.858	2.221
1.778	0.2100	0.4085	0.838	1.768	0.868	2.068
1.669	0.2315	0.4455	0.828	1.669	0.875	1.936
1.569	0.2456	0.4800	0.782	1.599	0.801	1.820
1.500	0.2483	0.4985	0.748	1.499	0.748	1.720
1.390	0.2495	0.4965	0.699	1.390	0.699	1.598
1.311	0.2484	0.4945	0.661	1.307	0.637	1.484
1.221	0.2502	0.4975	0.618	1.204	0.587	1.371
1.122	0.2535	0.4975	0.572	1.087	0.546	1.276
1.033	0.2568	0.5005	0.530	1.023	0.505	1.174
0.936	0.2587	0.5024	0.483	0.932	0.478	1.068
0.856	0.2607	0.5062	0.441	0.858	0.443	0.981
0.749	0.2635	0.5160	0.383	0.754	0.378	0.840
0.671	0.2650	0.5200	0.342	0.674	0.344	0.768
0.552	0.2689	0.5265	0.282	0.548	0.282	0.623

TABLE NO. 4

Six-Blade Propeller  
 $\beta = 65^\circ$

Small Spinner  
Plain Blade Roots

Test No. 9						
V/ND	C <sub>T</sub>	C <sub>P</sub>	$\eta$	C <sub>S</sub>	$\eta$	C <sub>S</sub>
4.151	0.2549	1.406	0.752	3.886	0.750	3.920
3.960	0.2772	1.459	0.764	3.685	0.765	3.765
3.772	0.2995	1.461	0.774	3.510	0.766	3.620
3.633	0.3122	1.477	0.787	3.372	0.770	3.448
3.453	0.3300	1.492	0.769	3.200	0.770	3.278
3.282	0.3335	1.476	0.743	3.047	0.758	3.105
3.138	0.3250	1.429	0.712	2.924	0.730	2.989
2.940	0.3112	1.353	0.673	2.762	0.684	2.819
2.800	0.2975	1.294	0.644	2.680	0.665	2.725
2.631	0.2840	1.227	0.609	2.527	0.624	2.592
2.472	0.2705	1.167	0.574	2.399	0.586	2.441
2.292	0.2606	1.115	0.536	2.250	0.553	2.320
2.135	0.2520	1.073	0.502	2.110	0.516	2.170
1.960	0.2392	1.034	0.455	1.949	0.482	2.040
1.826	0.2335	1.009	0.423	1.826	0.443	1.904
1.634	0.2249	0.987	0.372	1.635	0.401	1.750
1.505	0.2159	0.972	0.359	1.515	0.360	1.600
1.311	0.2110	0.955	0.289	1.325	0.279	1.460
1.156	0.2070	0.935	0.252	1.173	0.233	1.285
1.003	0.1995	0.924	0.217	1.019	0.202	1.097

TABLE NO. 3

Six-Blade Propeller  
 $\beta = 55^\circ$

Small Spinner  
Plain Blade Roots

Test No. 6						
V/ND	C <sub>T</sub>	C <sub>P</sub>	$\eta$	C <sub>S</sub>	$\eta$	C <sub>S</sub>
2.990	0.1635	0.6130	0.795	3.284	0.801	3.272
2.844	0.1901	0.6660	0.811	3.086	0.808	3.125
2.732	0.2113	0.7061	0.817	2.929	0.822	2.956
2.615	0.2325	0.7405	0.820	2.780	0.822	2.790
2.491	0.2519	0.7660	0.820	2.630	0.819	2.648
2.360	0.2696	0.7945	0.800	2.476	0.806	2.487
2.244	0.2745	0.8020	0.768	2.345	0.774	2.362
2.129	0.2739	0.7945	0.734	2.233	0.741	2.254
2.010	0.2699	0.7773	0.698	2.115	0.704	2.125
1.884	0.2652	0.7580	0.660	1.995	0.663	2.012
1.773	0.2615	0.7420	0.624	1.883	0.624	1.883
1.650	0.2617	0.7360	0.587	1.756	0.582	1.750
1.540	0.2599	0.7310	0.548	1.642	0.554	1.657
1.434	0.2565	0.7180	0.470	1.406	0.507	1.523
1.337	0.2553	0.7175	0.423	1.272	0.473	1.416
1.249	0.2563	0.7210	0.388	1.164	0.421	1.285
1.169	0.2563	0.7278	0.332	1.066	0.385	1.165
1.092	0.2563	0.7278	0.292	0.989	0.339	1.026
0.932	0.2552	0.7278	0.232	0.889	0.289	0.880
0.825	0.2540	0.7210	0.256	0.775	0.252	0.769
0.725	0.2540	0.7210	0.256	0.654	0.252	0.769
0.623	0.2582	0.7221	0.508	1.517	0.335	1.019

TABLE NO. 5

Six-Blade Prop. Small Spinner  
 $\beta = 45^\circ$  Paired Blade Roots

Six-Blade Prop. Small Spinner  
 $\beta = 65^\circ$  Paired Blade Roots

Test No. 12						
V/ND	C <sub>T</sub>	C <sub>P</sub>	$\eta$	C <sub>S</sub>	$\eta$	C <sub>S</sub>
2.326	0.0567	0.2136	0.619	3.400	0.796	3.829
2.225	0.0924	0.2754	0.747	2.879	0.798	3.871
2.127	0.1221	0.3209	0.808	2.672	0.798	3.510
2.047	0.1448	0.3558	0.836	2.519	0.796	3.350
1.957	0.1694	0.3902	0.851	2.360	0.786	3.185
1.857	0.1963	0.4244	0.860	2.203	0.759	3.036
1.769	0.2168	0.4494	0.854	2.072	0.728	2.910
1.689	0.2341	0.4708	0.831	1.935	0.691	2.786
1.570	0.2484	0.4968	0.786	1.804	0.652	2.683
1.480	0.2518	0.5042	0.695	1.693	0.617	2.580
1.381	0.2521	0.5019	0.595	1.583	0.576	2.371
1.291	0.2519	0.4977	0.654	1.483		
1.182	0.2535	0.5080	0.602	1.350		

TABLE NO. 6

Six-Blade Prop. Small Spinner  
 $\beta = 65^\circ$  Paired Blade Roots

Test No. 11B						
V/ND	C <sub>T</sub>	C <sub>P</sub>	$\eta$	C <sub>S</sub>	$\eta$	C <sub>S</sub>
4.082	0.2719	1.393	0.796	3.829		
3.937	0.2880	1.423	0.798	3.871		
3.767	0.3060	1.448	0.798	3.510		
3.606	0.3230	1.464	0.796	3.350		
3.432	0.3370	1.472	0.786	3.185		
3.269	0.3400	1.464	0.759	3.036		
3.120	0.3338	1.429	0.728	2.910		
2.940	0.3180	1.353	0.691	2.786		
2.771	0.3022	1.283	0.652	2.683		
2.625	0.2890	1.228	0.617	2.580		
2.443	0.2760	1.170	0.576	2.371		

TABLE NO. 8

Six-Blade Propeller  
 $\beta = 45^\circ$

Large Spinner  
Spinner Apertures Closed

Test No. 13									
V/ND	C <sub>T</sub>	C <sub>P</sub>	$\eta$	C <sub>S</sub>	V/ND	C <sub>T</sub>	C <sub>P</sub>	$\eta$	C <sub>S</sub>
1.643	0.0300	0.1003	0.493	2.605	1.605	0.0510	0.1220	0.670	2.448
1.569	0.0636	0.1375	0.726	2.335	1.540	0.0769	0.1541	0.770	2.238
1.507	0.0998	0.1701	0.842	2.146	1.457	0.1079	0.1902	0.826	2.030
1.444	0.1338	0.1981	0.826	1.995	1.394	0.1298	0.2134	0.842	1.898
1.370	0.1553	0.2209	0.840	1.851	1.319	0.1509	0.2372	0.841	1.758
1.304	0.1642	0.2397	0.840	1.738	1.257	0.1691	0.2535	0.839	1.655
1.247	0.1662	0.2516	0.843	1.606	1.193	0.1853	0.2676	0.826	1.554
1.187	0.1674	0.2616	0.828	1.493	1.117	0.2043	0.2832	0.806	1.440
1.127	0.1646	0.2768	0.813	1.403	1.041	0.2212	0.2965	0.777	1.351
1.060	0.1577	0.2913	0.792	1.299	0.966	0.2342	0.3041	0.759	1.253
1.000	0.1401	0.3097	0.734	1.199	0.906	0.2408	0.3152	0.692	1.141
0.938	0.1240	0.3111	0.727	1.185	0.851	0.2406	0.3193	0.642	1.072
0.874	0.1085	0.3185	0.660	1.100	0.778	0.2441	0.3201	0.593	0.903
0.805	0.0927	0.3199	0.611	1.011	0.719	0.2451	0.3217	0.548	0.821
0.744	0.0744	0.3206	0.565	0.933	0.656	0.2447	0.3256	0.494	0.724
0.673	0.0542	0.3245	0.506	0.843	0.579	0.2478	0.3300	0.436	0.634
0.612	0.0412	0.3284	0.463	0.765	0.508	0.2511	0.3333	0.384	0.563
0.540	0.0292	0.3321	0.406	0.674	0.453	0.2543	0.3367	0.342	0.507
0.483	0.0244	0.3352	0.346	0.602	0.408	0.2559	0.3406	0.307	0.507

TABLE NO. 7

Six-Blade Propeller  
 $\beta = 35^\circ$

Large Spinner  
Spinner Apertures Closed

Test No. 20									
V/ND	C <sub>T</sub>	C <sub>P</sub>	$\eta$	C <sub>S</sub>	V/ND	C <sub>T</sub>	C <sub>P</sub>	$\eta$	C <sub>S</sub>
1.643	0.0300	0.1003	0.493	2.605	1.605	0.0510	0.1220	0.670	2.448
1.569	0.0636	0.1375	0.726	2.335	1.540	0.0769	0.1541	0.770	2.238
1.507	0.0998	0.1701	0.842	2.146	1.457	0.1079	0.1902	0.826	2.030
1.444	0.1338	0.1981	0.826	1.995	1.394	0.1298	0.2134	0.842	1.898
1.370	0.1553	0.2209	0.840	1.851	1.319	0.1509	0.2372	0.841	1.758
1.304	0.1642	0.2397	0.840	1.738	1.257	0.1691	0.2535	0.839	1.655
1.247	0.1662	0.2516	0.843	1.606	1.193	0.1853	0.2676	0.826	1.554
1.187	0.1674	0.2616	0.828	1.493	1.117	0.2043	0.2832	0.806	1.440
1.127	0.1646	0.2768	0.813	1.403	1.041	0.2212	0.2965	0.777	1.351
1.060	0.1577	0.2913	0.792	1.299	0.966	0.2342	0.3041	0.759	1.253
1.000	0.1401	0.3097	0.734	1.199	0.906	0.2408	0.3152	0.692	1.141
0.938	0.1240	0.3111	0.727	1.185	0.851	0.2406	0.3193	0.642	1.072
0.874	0.1085	0.3185	0.660	1.100	0.778	0.2441	0.3201	0.593	0.903
0.805	0.0927	0.3199	0.611	1.011	0.719	0.2451	0.3217	0.548	0.821
0.744	0.0744	0.3206	0.565	0.933	0.656	0.2447	0.3256	0.494	0.724
0.673	0.0542	0.3245	0.506	0.843	0.579	0.2478	0.3300	0.436	0.634
0.612	0.0412	0.3284	0.463	0.765	0.508	0.2511	0.3333	0.384	0.563
0.540	0.0292	0.3321	0.406	0.674	0.453	0.2543	0.3367	0.342	0.507
0.483	0.0244	0.3352	0.346	0.602	0.408	0.2559	0.3406	0.307	0.507

TABLE NO. 9

Six-Blade Propeller  
 $\beta = 55^\circ$

Large Spinner  
Spinner Apertures Closed

Test No. 18									
V/ND	C <sub>T</sub>	C <sub>P</sub>	$\eta$	C <sub>S</sub>	V/ND	C <sub>T</sub>	C <sub>P</sub>	$\eta$	C <sub>S</sub>
2.967	0.1555	0.5750	0.800	3.320	3.013	0.1449	0.5565	0.784	3.387
2.862	0.1772	0.6192	0.820	3.148	2.917	0.1673	0.5960	0.819	3.238
2.730	0.2071	0.6730	0.841	2.954	2.791	0.1931	0.6480	0.834	3.042
2.600	0.2327	0.7160	0.845	2.782	2.665	0.2190	0.6920	0.843	2.873
2.499	0.2491	0.7440	0.836	2.651	2.550	0.2390	0.7220	0.844	2.726
2.367	0.2690	0.7675	0.830	2.500	2.436	0.2603	0.7550	0.840	2.582
2.252	0.2770	0.7860	0.794	2.365	2.309	0.2755	0.7790	0.816	2.427
2.132	0.2775	0.7810	0.758	2.240	2.203	0.2791	0.7860	0.783	2.313
2.021	0.2746	0.7620	0.718	2.149	2.071	0.2770	0.7890	0.745	2.185
1.892	0.2690	0.7440	0.684	2.007	1.949	0.2744	0.7542	0.708	2.066
1.773	0.2671	0.7299	0.648	1.892	1.840	0.2699	0.7390	0.671	1.956
1.644	0.2635	0.7140	0.608	1.759	1.709	0.2658	0.7230	0.632	1.827
1.543	0.2635	0.7075	0.522	1.652	1.587	0.2641	0.7170	0.585	1.691
1.412	0.2613	0.7057	0.479	1.551	1.456	0.2638	0.7120	0.551	1.601
1.298	0.2593	0.7038	0.430	1.451	1.367	0.2609	0.7070	0.504	1.464
1.191	0.2570	0.7018	0.397	1.348	1.243	0.2578	0.7060	0.455	1.334
1.072	0.2569	0.7059	0.330	1.248	1.128	0.2570	0.7082	0.412	1.207
0.972	0.2575	0.7100	0.299	1.040	1.005	0.2570	0.7140	0.367	0.974
0.834	0.2563	0.7160	0.248	0.892	0.910	0.2570	0.7140	0.327	0.825
0.695	0.2560	0.7180	0.248	0.744	0.770	0.2571	0.7170	0.276	0.625

TABLE NO. 10

Six-Blade Propeller  
 $\beta = 65^\circ$

Large Spinner  
Spinner Apertures Closed

Test No. 15									
V/ND	C <sub>T</sub>	C <sub>P</sub>	$\eta$	C <sub>S</sub>	V/ND	C <sub>T</sub>	C <sub>P</sub>	$\eta$	C <sub>S</sub>
4.130	0.2430	1.302	0.771	3.917	4.091	0.2481	1.306	0.777	3.881
3.960	0.2645	1.333	0.736	3.739	3.940	0.2676	1.334	0.790	3.720
3.795	0.2850	1.368	0.702	3.568	3.772	0.2866	1.370	0.795	3.550
3.622	0.3060	1.385	0.708	3.400	3.601	0.3070	1.400	0.793	3.375
3.455	0.3193	1.403	0.768	3.238	3.430	0.3220	1.405	0.786	3.211
3.295	0.3295	1.405	0.773	3.089	3.259	0.3289	1.399	0.766	3.052
3.118	0.3221	1.367	0.734	2.931	3.095	0.3200	1.383	0.726	2.903
2.950	0.3125	1.316	0.700	2.794	2.894	0.3073	1.295	0.688	2.747
2.790	0.2993	1.248	0.639	2.673	2.721	0.2904	1.222	0.648	2.615
2.643	0.2925	1.187	0.592	2.556	2.570	0.2760	1.165	0.609	2.492
2.433	0.2670	1.117	0.552	2.384	2.398	0.2654	1.110	0.574	2.350
2.303	0.2604	1.082	0.555	2.273	2.300	0.2590	1.079	0.552	2.270
2.115	0.2476	1.035	0.511	2.107	2.083	0.2460	1.027	0.498	2.073
1.970	0.2385	0.982	0.474	1.972	1.910	0.2360	0.990	0.455	1.912
1.813	0.2308	0.969	0.432	1.823	1.752	0.2280	0.962	0.416	1.768
1.664	0.2259	0.944	0.394	1.681	1.575	0.2229	0.948	0.370	1.590
1.487	0.2229	0.947	0.350	1.505	1.740	0.2281	0.961	0.313	1.413
1.325	0.2228	0.951	0.310	1.339	1.391	0.2207	0.943	0.325	1.402
1.187	0.2210	0.942	0.279	1.200	1.198	0.2184	0.938	0.279	1.214
0.966	0.2131	0.917	0.225	1.015	0.976	0.2137	0.916	0.228	0.993

Tables 7, 8, 9, 10

TABLE NO. 11

TABLE NO. 12

TABLE NO. 13

Six-Blade Propeller $\beta = 45^\circ$	Large Spinner Spinner Apertures Open	Six-Blade Propeller $\beta = 65^\circ$	Large Spinner Spinner Apertures Open	Four-Blade Propeller $\beta = 35^\circ$	Small Spinner Plain Blade Roots
---	---	---	---	--	------------------------------------

Test No. 22

Test No. 17

Test No. 30

V/nD	C <sub>T</sub>	C <sub>P</sub>	$\eta$	C <sub>S</sub>	V/nD	C <sub>T</sub>	C <sub>P</sub>	$\eta$	C <sub>S</sub>	V/nD	C <sub>T</sub>	C <sub>P</sub>	$\eta$	C <sub>S</sub>
2.325	0.0452	0.1944	0.540	3.223	4.110	0.2211	1.282	0.709	3.909	1.618	0.0346	0.0960	0.651	2.622
2.236	0.0766	0.2483	0.690	2.955	4.000	0.2350	1.310	0.716	3.790	1.532	0.0586	0.1159	0.775	2.589
2.136	0.1064	0.2968	0.765	2.730	3.785	0.2572	1.345	0.725	3.560	1.470	0.0752	0.1341	0.824	2.501
2.058	0.1297	0.3333	0.800	2.570	3.655	0.2740	1.368	0.731	3.435	1.396	0.0920	0.1525	0.842	2.034
1.945	0.1609	0.3780	0.828	2.363	3.489	0.2913	1.377	0.738	3.272	1.329	0.1069	0.1679	0.844	1.899
1.862	0.1822	0.4060	0.836	2.233	3.300	0.3041	1.383	0.726	3.099	1.264	0.1210	0.1822	0.840	1.777
1.761	0.2050	0.4344	0.830	2.079	3.145	0.3025	1.367	0.696	2.956	1.200	0.1337	0.1933	0.830	1.667
1.669	0.2249	0.4560	0.822	1.950	2.985	0.2930	1.309	0.668	2.830	1.129	0.1482	0.2040	0.820	1.551
1.573	0.2364	0.4756	0.790	1.825	2.817	0.2773	1.240	0.629	2.704	1.061	0.1589	0.2110	0.798	1.448
1.475	0.2439	0.4939	0.734	1.697						0.991	0.1714	0.2198	0.773	1.341
1.386	0.2451	0.4850	0.700	1.596						0.914	0.1706	0.2262	0.689	1.231
1.291	0.2451	0.4921	0.657	1.490						0.860	0.1721	0.2272	0.654	1.157
1.171	0.2460	0.4940	0.596	1.352						0.790	0.1731	0.2287	0.598	1.061
										0.710	0.1755	0.2328	0.536	0.951
										0.658	0.1789	0.2371	0.496	0.877
										0.574	0.1805	0.2399	0.432	0.763
										0.522	0.1829	0.2420	0.394	0.694
										0.448	0.1853	0.2460	0.337	0.593

TABLE NO. 14

TABLE NO. 15

Four-Blade Propeller $\beta = 45^\circ$	Small Spinner Plain Blade Roots	Four-Blade Propeller $\beta = 55^\circ$	Small Spinner Plain Blade Roots
--	------------------------------------	--	------------------------------------

Test No. 26

Test No. 27

Test No. 31

Test No. 32

V/nD	C <sub>T</sub>	C <sub>P</sub>	$\eta$	C <sub>S</sub>	V/nD	C <sub>T</sub>	C <sub>P</sub>	$\eta$	C <sub>S</sub>	V/nD	C <sub>T</sub>	C <sub>P</sub>	$\eta$	C <sub>S</sub>
2.363	0.0276	0.1828	0.530	3.596	2.340	0.0373	0.1410	0.619	3.466	2.999	0.1132	0.4280	0.783	3.539
2.270	0.0540	0.1993	0.724	3.239	2.233	0.0647	0.1865	0.775	3.124	2.863	0.1306	0.4608	0.812	3.341
2.168	0.0781	0.2105	0.804	2.961	2.138	0.0847	0.2210	0.819	2.888	2.750	0.1473	0.4930	0.822	3.065
2.079	0.0966	0.2396	0.838	2.765	2.050	0.1036	0.2490	0.853	2.706	2.638	0.1617	0.5180	0.824	2.814
1.972	0.1184	0.2707	0.862	2.564	1.960	0.1206	0.2752	0.859	2.540	2.490	0.1795	0.5430	0.824	2.583
1.883	0.1349	0.2940	0.864	2.408	1.854	0.1393	0.2985	0.862	2.364	2.360	0.1993	0.5590	0.802	2.346
1.785	0.1507	0.3140	0.856	2.251	1.760	0.1551	0.3195	0.854	2.214	2.269	0.1910	0.5610	0.772	2.157
1.700	0.1629	0.3300	0.843	2.127	1.665	0.1686	0.3345	0.839	2.076	2.157	0.1904	0.5584	0.734	2.023
1.564	0.1753	0.3440	0.807	1.964	1.557	0.1755	0.3490	0.748	1.926	2.002	0.1874	0.5420	0.698	1.908
1.490	0.1757	0.3490	0.750	1.842	1.480	0.1765	0.3495	0.698	1.828	1.908	0.1845	0.5322	0.661	1.777
1.397	0.1770	0.3470	0.712	1.729	1.359	0.1776	0.3466	0.666	1.682	1.777	0.1810	0.5183	0.620	1.663
1.301	0.1779	0.3465	0.658	1.612	1.294	0.1783	0.3466	0.614	1.503	1.663	0.1784	0.5100	0.582	1.556
1.215	0.1797	0.3482	0.598	1.503	1.191	0.1792	0.3467	0.560	1.472	1.556	0.1782	0.5115	0.543	1.447
1.129	0.1808	0.3505	0.532	1.394	1.086	0.1820	0.3529	0.514	1.338	1.530	0.1792	0.5097	0.503	1.322
1.035	0.1829	0.3552	0.459	1.275	0.992	0.1840	0.3549	0.454	1.220	1.502	0.1791	0.5062	0.484	1.207
0.942	0.1950	0.3669	0.489	1.159	0.887	0.1854	0.3580	0.409	1.152	1.322	0.1779	0.5114	0.425	1.078
0.854	0.1970	0.3610	0.443	1.049	0.791	0.1893	0.3660	0.374	0.970	1.207	0.1791	0.5160	0.378	0.976
0.724	0.1910	0.3700	0.374	0.883	0.675	0.1927	0.3730	0.349	0.833	1.078	0.1800	0.5183	0.338	0.833
0.660	0.1922	0.3741	0.339	0.805	0.597	0.1948	0.3780	0.307	0.725	0.976	0.1796	0.5150	0.299	0.778
0.542	0.1955	0.3905	0.278	0.657						0.853	0.1782	0.5180	0.235	0.683

Tables 11, 12, 13, 14, 15

TABLE NO. 16

Four-Blade Propeller  $\beta = 65^\circ$  Small Spinner  
Plain Blade Roots

Test No. 33

V/ND	C <sub>T</sub>	C <sub>P</sub>	$\eta$	C <sub>S</sub>	V/ND	C <sub>T</sub>	C <sub>P</sub>	$\eta$	C <sub>S</sub>
4.183	0.1748	0.974	0.751	4.208	4.220	0.1705	0.988	0.743	4.240
3.990	0.1908	0.998	0.763	3.990	4.060	0.1844	0.993	0.753	4.065
3.680	0.2155	1.036	0.766	3.658	3.890	0.1995	1.012	0.766	3.885
3.483	0.2317	1.048	0.770	3.455	3.700	0.2145	1.032	0.769	3.682
3.840	0.2040	1.021	0.768	3.832	3.560	0.2250	1.043	0.769	3.530
3.293	0.2318	1.032	0.740	3.277	3.358	0.2332	1.043	0.750	3.329
3.105	0.2228	0.987	0.700	3.110	3.185	0.2276	1.015	0.715	3.185
2.811	0.2060	0.953	0.674	2.867	3.040	0.2198	0.973	0.662	3.050
2.640	0.1952	0.855	0.602	2.722	2.700	0.1990	0.889	0.618	2.780
2.478	0.1845	0.808	0.566	2.585	2.560	0.1883	0.828	0.584	2.662
2.330	0.1771	0.777	0.531	2.451	2.397	0.1799	0.793	0.546	2.505
2.142	0.1700	0.743	0.490	2.273	2.190	0.1707	0.750	0.499	2.320
1.987	0.1626	0.719	0.449	2.126	2.071	0.1656	0.730	0.470	2.210
1.825	0.1565	0.697	0.410	1.962	1.885	0.1571	0.703	0.422	2.025
1.645	0.1535	0.690	0.366	1.775	1.694	0.1533	0.694	0.374	1.824
1.495	0.1475	0.679	0.325	1.616	1.566	0.1513	0.688	0.347	1.690
1.338	0.1410	0.670	0.282	1.449	1.432	0.1422	0.678	0.290	1.495
1.162	0.1370	0.663	0.241	1.263	1.245	0.1300	0.663	0.259	1.352
.982	0.1362	0.656	0.204	1.062	1.107	0.1362	0.655	0.230	1.206

TABLE NO. 18

Four-Blade Propeller  $\beta = 65^\circ$  Small Spinner  
Faired Blade Roots

Test No. 35

V/ND	C <sub>T</sub>	C <sub>P</sub>	$\eta$	C <sub>S</sub>
4.135	0.1870	0.985	0.784	4.147
4.006	0.1980	1.000	0.792	4.006
3.825	0.2124	1.028	0.790	3.813
3.670	0.2260	1.044	0.794	3.644
3.460	0.2375	1.047	0.784	3.432
3.295	0.2370	1.035	0.754	3.277
3.200	0.2319	1.015	0.732	3.197
2.955	0.2190	0.948	0.683	2.986
2.773	0.2075	0.894	0.643	2.834
2.631	0.1975	0.852	0.613	2.718
2.450	0.1865	0.807	0.566	2.558

TABLE NO. 17

Four-Blade Propeller  $\beta = 45^\circ$  Small Spinner  
Faired Blade Roots

Test No. 38

V/ND	C <sub>T</sub>	C <sub>P</sub>	$\eta$	C <sub>S</sub>
2.325	0.0409	0.1411	0.674	3.441
2.240	0.0650	0.1836	0.792	3.143
2.148	0.0860	0.2203	0.838	2.906
2.053	0.1044	0.2487	0.862	2.710
1.948	0.1236	0.2763	0.871	2.519
1.855	0.1396	0.2980	0.868	2.365
1.764	0.1550	0.3185	0.868	2.221
1.684	0.1775	0.3470	0.810	1.963
1.679	0.1687	0.3332	0.849	2.095
1.480	0.1775	0.3495	0.752	1.828
1.389	0.1789	0.3495	0.711	1.715
1.300	0.1807	0.3500	0.672	1.604

TABLE NO. 19

Six-Blade Dual Rotation Propeller  $\beta_{RH} = 55^\circ$   $\beta_{LH} = 34.3^\circ$  Small Spinner  
Plain Blade Roots

Test No. 42

V/ND	C <sub>T</sub>	C <sub>P</sub>	$\eta$	C <sub>S</sub>
1.653	0.0437	0.1262	0.0086	2.503
1.593	0.0756	0.1599	0.0067	2.297
1.510	0.1080	0.1977	0.0031	2.088
1.439	0.1315	0.2242	-	1.940
1.370	0.1611	0.2563	-	1.798
1.312	0.1805	0.2760	-	1.700
1.244	0.2019	0.2974	-	1.589
1.164	0.2258	0.3166	-	1.467
1.093	0.2455	0.3307	-	1.366
1.027	0.2656	0.3435	-	1.285
0.964	0.2784	0.3562	-	1.187
0.890	0.2865	0.3650	-	1.089
0.821	0.2920	0.3740	-	1.000
0.757	0.2931	0.3813	-	0.918
0.696	0.3030	0.3965	-	0.842
0.628	0.3062	0.3922	-	0.757
0.578	0.3098	0.3970	-	0.694
0.494	0.3187	0.4073	-	0.592
0.413	0.3240	0.4140	-	0.323

Test No. 49

V/ND	C <sub>T</sub>	C <sub>P</sub>	$\eta$	C <sub>S</sub>
1.624	0.0621	0.1443	0.0067	2.898
1.536	0.0972	0.1854	0.0039	2.150
1.470	0.1218	0.2146	-	1.999
1.404	0.1516	0.2477	-	1.855
1.338	0.1720	0.2690	-	1.742
1.270	0.1932	0.2883	-	1.629
1.205	0.2133	0.3087	-	1.528
1.121	0.2375	0.3260	-	1.403
1.060	0.2556	0.3385	-	1.317
0.984	0.2743	0.3520	-	1.222
0.916	0.2833	0.3647	-	1.121
0.857	0.2889	0.3691	-	1.046
0.789	0.2941	0.3785	-	0.964
0.714	0.3018	0.3868	-	0.864
0.652	0.3054	0.3905	-	0.787
0.584	0.3089	0.3970	-	0.701
0.512	0.3159	0.4060	-	0.614
0.460	0.3210	0.4100	-	0.550

Tables 16, 17, 18, 19

Six-Blade Dual Rotation Propeller  
 $\beta_{RH} = 45^\circ$   $\beta_{LH} = 43.6^\circ$   
 Small Spinner  
 Plain Blade Roots

Test No. 50						Test No. 51					
V/nD	C <sub>T</sub>	C <sub>P</sub>	$\Delta C_P$	$\eta$	C <sub>S</sub>	V/nD	C <sub>T</sub>	C <sub>P</sub>	$\Delta C_P$	$\eta$	C <sub>S</sub>
2.329	0.0555	0.2192	0.0191	0.568	3.154	2.293	0.0730	0.2452	0.0172	0.688	3.063
2.241	.0942	.2793	.0132	.756	2.891	2.201	.1094	.3086	.0082	.780	2.791
2.160	.1220	.3272	.0085	.806	2.702	2.089	.1476	.3680	.0037	.837	2.550
2.082	.1566	.3815	.0031	.842	2.490	2.001	.1725	.4070	.0034	.848	2.400
1.960	.1845	.4230	- .0003	.855	2.341	1.902	.2030	.4470	- .0041	.864	2.230
1.859	.2151	.4663	- .0034	.858	2.160	1.820	.2277	.4815	- .0048	.860	2.100
1.773	.2404	.4984	- .0079	.855	2.034	1.728	.2534	.5115	- .0089	.856	1.972
1.678	.2622	.5212	- .0088	.844	1.910	1.638	.2749	.5355	- .0137	.841	1.852
1.580	.2822	.5450	- .0119	.818	1.801	1.528	.2888	.5555	- .0177	.794	1.716
1.493	.2944	.5625	- .0213	.782	1.673	1.446	.2988	.5671	- .0273	.762	1.620
1.386	.3010	.5715	- .0308	.730	1.550	1.353	.3020	.5705	- .0338	.716	1.515
1.301	.3028	.5730	- .0354	.687	1.456	1.238	.3050	.5725	- .0342	.659	1.385
1.214	.3070	.5745	- .0365	.649	1.357	1.171	.3091	.5765	- .0378	.628	1.250
1.120	.3100	.5795	- .0380	.599	1.250	1.076	.3122	.5790	- .0364	.580	1.201
1.033	.3145	.5855	- .0367	.554	1.148	.966	.3177	.5875	- .0372	.522	1.074
.930	.3200	.5905	- .0397	.510	1.033	.886	.3224	.5930	- .0382	.482	.984
.846	.3238	.5940	- .0393	.461	.939	.794	.3276	.5990	- .0426	.434	.880
.775	.3281	.6014	- .0404	.425	.857	.685	.3327	.6085	- .0421	.368	.755
.660	.3332	.6120	- .0427	.359	.727	.596	.3371	.6200	- .0420	.324	.656
.582	.3360	.6210	- .0437	.315	.639						

TABLE NO. 21

Six-Blade Dual Rotation Propeller  
 $\beta_{RH} = 55^\circ$   $\beta_{LH} = 53.1^\circ$   
 Small Spinner  
 Plain Blade Roots

Test No. 53						Test No. 54					
V/nD	C <sub>T</sub>	C <sub>P</sub>	$\Delta C_P$	$\eta$	C <sub>S</sub>	V/nD	C <sub>T</sub>	C <sub>P</sub>	$\Delta C_P$	$\eta$	C <sub>S</sub>
3.002	0.1814	0.6612	0.0250	0.824	3.266	3.030	0.1755	0.6420	0.0237	0.826	3.309
2.889	.2084	.7154	.0198	.842	3.091	2.938	.1993	.6965	.0158	.841	3.170
2.783	.2369	.7658	.0096	.861	2.939	2.840	.2235	.7390	.0090	.859	3.019
2.636	.2674	.8180	.0000	.862	2.741	2.690	.2566	.7990	.0028	.864	2.819
2.522	.2919	.8663	- .0028	.859	2.598	2.562	.2829	.8415	- .0034	.862	2.654
2.392	.3137	.8860	- .0090	.847	2.447	2.448	.3067	.8720	- .0119	.861	2.519
2.275	.3269	.9041	- .0220	.822	2.321	2.326	.3252	.9000	- .0158	.841	2.373
2.155	.3328	.9053	- .0372	.792	2.198	2.210	.3315	.9080	- .0275	.807	2.254
2.025	.3308	.9009	- .0478	.744	2.066	2.095	.3320	.9015	- .0403	.772	2.137
1.912	.3292	.8845	- .0536	.712	1.960	1.960	.3300	.8855	- .0532	.731	2.007
1.791	.3248	.8673	- .0498	.678	1.845	1.865	.3296	.8785	- .0529	.699	1.915
1.668	.3205	.8518	- .0528	.628	1.723	1.725	.3259	.8615	- .0503	.644	1.777
1.560	.3186	.8426	- .0506	.590	1.615	1.600	.3215	.8465	- .0511	.608	1.654
1.437	.3172	.8460	- .0519	.539	1.487	1.499	.3195	.8415	- .0512	.570	1.553
1.319	.3139	.8422	- .0529	.491	1.365	1.381	.3174	.8375	- .0545	.523	1.432
1.202	.3141	.8417	- .0505	.449	1.244	1.235	.3152	.8375	- .0526	.465	1.281
1.091	.3156	.8488	- .0485	.406	1.128	1.140	.3155	.8400	- .0496	.428	1.181
.989	.3106	.8490	- .0543	.362	1.022	1.009	.3130	.8460	- .0495	.374	1.043
.847	.3091	.8522	- .0613	.307	.874	.914	.3102	.8425	- .0588	.336	.946
.697	.3115	.8693	- .0732	.250	.718	.778	.3120	.8560	- .0678	.284	.802

TABLE NO. 22

Six-Blade Dual Rotation Propeller  
 $\beta_{RH} = 65^\circ$   $\beta_{LH} = 62.5^\circ$   
 Small Spinner  
 Plain Blade Roots

Test No. 60						Test No. 61					
V/nD	C <sub>T</sub>	C <sub>P</sub>	$\Delta C_P$	$\eta$	C <sub>S</sub>	V/nD	C <sub>T</sub>	C <sub>P</sub>	$\Delta C_P$	$\eta$	C <sub>S</sub>
4.145	0.3139	1.531	0.0347	0.850	3.822	4.130	0.3129	1.532	+0.0354	0.844	3.805
3.980	.2420	1.590	.0225	.856	3.620	3.981	.3420	1.585	.0193	.859	3.623
3.820	.3630	1.615	.0107	.858	3.470	3.810	.3629	1.611	.0107	.858	3.470
3.636	.3870	1.639	.0000	.859	3.300	3.640	.3968	1.643	.0000	.856	3.294
3.470	.4075	1.655	- .0118	.855	3.135	3.460	.4078	1.651	- .0128	.854	3.130
3.300	.4172	1.645	- .0257	.838	2.988	3.283	.4175	1.641	- .0300	.836	2.975
3.134	.4165	1.614	- .0491	.809	2.850	3.155	.4170	1.618	- .0500	.813	2.867
2.990	.4070	1.567	- .0617	.778	2.730	2.993	.4073	1.565	- .0653	.779	2.739
2.812	.3900	1.489	- .0757	.737	2.602	2.807	.3870	1.482	- .0765	.733	2.600
2.650	.3715	1.416	- .0743	.695	2.474	2.630	.3692	1.400	- .0760	.694	2.461
2.465	.3493	1.334	- .0730	.646	2.297	2.462	.3478	1.320	- .0778	.642	2.325
2.300	.3307	1.267	- .0606	.600	2.194	2.311	.3316	1.266	- .0710	.605	2.209
2.131	.2966	1.181	- .0679	.535	2.063	2.150	.3052	1.197	- .0677	.548	2.074
1.975	.2819	1.144	- .0594	.487	1.922	1.995	.2988	1.151	- .0530	.518	1.934
1.810	.2747	1.115	- .0593	.445	1.774	1.820	.2735	1.114	- .0641	.447	1.784
1.658	.2600	1.088	- .0639	.396	1.632	1.643	.2600	1.085	- .0685	.394	1.618
1.515	.2493	1.071	- .0648	.352	1.498	1.486	.2483	1.070	- .0695	.345	1.469
1.353	.2453	1.066	- .0640	.314	1.340	1.372	.2443	1.064	- .0660	.315	1.359
1.203	.2430	1.063	- .0616	.275	1.192	1.150	.2443	1.063	- .0640	.284	1.139
.996	.2460	1.073	- .0628	.228	.984	.998	.2470	1.078	- .0667	.229	.985

TABLE NO. 23

TABLE NO. 24 Tables 23, 24, 25, 26

Six-Blade Dual Rotation Propeller Small Spinner  
 $\beta_{RH} = 45^\circ$   $\beta_{LH} = 43.8^\circ$  Paired Blade Roots

Six-Blade Dual Rotation Propeller Small Spinner  
 $\beta_{RH} = 45^\circ$   $\beta_{LH} = 62.5^\circ$  Paired Blade Roots

Test No. 52

V/nD	$C_T$	$C_P$	$\Delta C_P$	$\eta$	$C_S$
2.334	0.0574	0.2090	0.0211	0.641	3.193
2.246	.0939	.2745	.0140	.768	2.906
2.155	.1277	.3319	.0110	.829	2.690
2.055	.1602	.3850	.0055	.855	2.488
1.952	.1916	.4318	.0017	.866	2.310
1.865	.2172	.4650	-.0048	.871	2.168
1.772	.2405	.4928	-.0069	.885	2.040
1.674	.2678	.5250	-.0075	.854	1.916
1.579	.2869	.5450	-.0118	.831	1.782
1.482	.2971	.5610	-.0223	.785	1.664
1.393	.3047	.5710	-.0324	.743	1.560
1.296	.3068	.5750	-.0346	.692	1.450

Test No. 62

V/nD	$C_T$	$C_P$	$\Delta C_P$	$\eta$	$C_S$
4.115	0.3235	1.551	+0.0299	0.858	3.767
3.965	.3489	1.568	+ .0161	.868	3.600
3.822	.3702	1.622	+ .0088	.873	3.470
3.631	.3959	1.654	- .0032	.870	3.283
3.486	.4147	1.662	- .0150	.864	3.125
3.270	.4247	1.654	- .0235	.840	2.955
3.131	.4222	1.810	- .0566	.819	2.848
2.986	.4133	1.574	- .0702	.794	2.721
2.804	.3932	1.486	- .0814	.742	2.595
2.637	.3736	1.406	- .0749	.700	2.462
2.461	.3547	1.334	- .0738	.655	2.322
2.300	.3323	1.268	- .0680	.604	2.192

TABLE NO. 25

Four-Blade Dual Rotation Propeller  
 $\beta_{RH} = 35^\circ$   $\beta_{LH} = 34.3^\circ$

Small Spinner  
 Plain Blade Roots

Test No. 41

V/nD	$C_T$	$C_P$	$\Delta C_P$	$\eta$	$C_S$
1.646	0.0318	0.0860	+0.0022	0.609	2.688
1.580	.0523	.1093	.0017	.758	2.483
1.506	.0740	.1335	.0016	.835	2.258
1.433	.0922	.1548	.0009	.853	2.080
1.358	.1090	.1718	.0005	.861	1.930
1.300	.1241	.1894	.0000	.852	1.810
1.227	.1390	.2006	-.0011	.850	1.692
1.162	.1544	.2134	-.0024	.842	1.583
1.086	.1685	.2222	-.0029	.824	1.486
1.018	.1799	.2317	-.0037	.791	1.362
.955	.1886	.2390	-.0040	.754	1.271
.887	.1960	.2451	-.0066	.709	1.175
.836	.1983	.2501	-.0089	.666	1.104
.752	.2017	.2541	-.0100	.596	.990
.683	.2043	.2590	-.0104	.539	.892
.626	.2047	.2606	-.0100	.489	.817
.568	.2098	.2660	-.0104	.447	.740
.483	.2142	.2673	-.0107	.387	.629
.420	.2183	.2732	-.0107	.336	.545

Test No. 50

V/nD	$C_T$	$C_P$	$\Delta C_P$	$\eta$	$C_S$
1.617	0.0409	0.0953	+0.0024	0.694	2.590
1.541	.0345	.1228	.0015	.808	2.348
1.478	.0828	.1448	.0018	.845	2.181
1.400	.0993	.1620	.0007	.861	2.014
1.333	.1175	.1806	-.0013	.867	1.878
1.271	.1314	.1935	-.0006	.863	1.764
1.200	.1465	.2080	-.0018	.845	1.643
1.125	.1522	.2182	-.0026	.836	1.524
1.059	.1757	.2270	-.0040	.820	1.424
.990	.1858	.2350	-.0037	.783	1.323
.919	.1944	.2437	-.0051	.733	1.220
.832	.1973	.2471	-.0080	.688	1.139
.794	.2002	.2520	-.0086	.631	1.046
.711	.2034	.2547	-.0100	.566	.935
.647	.2066	.2588	-.0100	.516	.848
.578	.2097	.2620	-.0102	.463	.756
.526	.2139	.2665	-.0104	.422	.685
.451	.2188	.2726	-.0108	.362	.585

TABLE NO. 26

Four-Blade Dual Rotation Propeller  
 $\beta_{RH} = 45^\circ$   $\beta_{LH} = 43.8^\circ$

Small Spinner  
 Plain Blade Roots

Test No. 38

V/nD	$C_T$	$C_P$	$\Delta C_P$	$\eta$	$C_S$
2.321	0.0408	0.1491	+0.0139	0.635	3.396
2.240	.0670	.1961	.0099	.765	3.100
2.151	.0868	.2285	.0075	.817	2.888
2.055	.1070	.2607	.0068	.844	2.690
1.947	.1290	.2912	.0044	.864	2.482
1.864	.1460	.3172	.0017	.858	2.349
1.762	.1653	.3390	.0000	.859	2.150
1.763	.1650	.3382	-.0003	.860	2.191
1.674	.1799	.3563	-.0024	.845	2.060
1.580	.1908	.3705	-.0051	.814	1.916
1.483	.1974	.3772	-.0088	.776	1.805
1.384	.2002	.3790	-.0132	.731	1.679
1.290	.2007	.3843	-.0129	.673	1.561
1.140	.2050	.3845	-.0125	.608	1.380
1.205	.2042	.3821	-.0138	.643	1.430
1.020	.2095	.3861	-.0122	.554	1.234
.932	.2122	.3896	-.0125	.508	1.125
.836	.2152	.3909	-.0148	.461	1.008
.766	.2176	.3977	-.0152	.419	.922
.688	.2196	.4073	-.0161	.355	.788
.564	.2205	.4169	-.0191	.298	.671

Test No. 39

V/nD	$C_T$	$C_P$	$\Delta C_P$	$\eta$	$C_S$
2.283	0.0510	0.1687	0.0119	0.691	3.265
2.199	.0757	.2120	.0109	.785	3.000
2.089	.0967	.2431	.0085	.830	2.773
1.990	.1195	.2779	.0084	.856	2.570
1.902	.1359	.3004	.0041	.860	2.420
1.800	.1576	.3267	.0024	.868	2.254
1.724	.1690	.3404	.0012	.856	2.140
1.627	.1837	.3583	-.0012	.834	2.000
1.525	.1939	.3711	-.0054	.796	1.861
1.441	.1988	.3763	-.0115	.761	1.755
1.343	.1994	.3760	-.0136	.712	1.635
1.243	.2021	.3805	-.0115	.660	1.506
1.170	.2044	.3805	-.0129	.629	1.418
1.069	.2065	.3822	-.0115	.577	1.295
.956	.2118	.3863	-.0121	.524	1.156
.880	.2144	.3914	-.0122	.482	1.063
.799	.2146	.3931	-.0129	.431	.962
.704	.2176	.4033	-.0114	.380	.846
.617	.2174	.4078	-.0140	.329	.739

TABLE NO. 27

Four-Blade Dual Rotation Propeller  
 $\beta_{RH} = 55^\circ$   $\beta_{LH} = 53.1^\circ$

Small Spinner  
 Plain Blade Roots

V/nD	C <sub>T</sub>	C <sub>P</sub>	$\Delta C_P$	$\eta$	C <sub>S</sub>
2.959	0.1208	0.4449	0.0268	0.803	3.473
2.883	.1362	.4730	.0221	.830	3.345
2.774	.1541	.5095	.0194	.839	3.170
2.632	.1735	.5428	.0135	.841	2.975
2.507	.1933	.5687	.0091	.852	2.801
2.408	.2033	.5840	.0049	.838	2.682
2.275	.2138	.6015	-.0032	.809	2.520
2.156	.2167	.6013	-.0096	.777	2.387
2.044	.2161	.5930	-.0139	.746	2.269
1.912	.2144	.5799	-.0160	.707	2.132
1.798	.2103	.5635	-.0164	.671	2.017
1.690	.2101	.5596	-.0161	.635	1.898
1.557	.2079	.5552	-.0167	.583	1.752
1.476	.2062	.5486	-.0173	.555	1.665
1.350	.2054	.5460	-.0161	.508	1.526
1.215	.2057	.5494	-.0166	.455	1.370
.996	.1983	.5512	-.0164	.360	1.123
.881	.1992	.5602	-.0195	.313	.990
.782	.1990	.5634	-.0217	.276	.876

TABLE NO. 28

Four-Blade Dual Rotation Propeller  
 $\beta_{RH} = 65^\circ$   $\beta_{LH} = 62.5^\circ$

Small Spinner  
 Plain Blade Roots

Test No. 47

V/nD	C <sub>T</sub>	C <sub>P</sub>	$\Delta C_P$	$\eta$	C <sub>S</sub>
4.195	0.1895	1.012	0.0636	0.786	4.190
4.078	.2041	1.039	.0498	.802	4.049
3.940	.2158	1.056	.0436	.805	3.901
3.730	.2367	1.082	.0325	.816	3.678
3.587	.2516	1.095	.0220	.824	3.522
3.421	.2620	1.100	.0132	.815	3.356
3.230	.2683	1.085	-.0011	.799	3.182
3.110	.2650	1.063	-.0134	.775	3.079
2.895	.2523	1.009	-.0205	.724	2.992
2.710	.2395	.945	-.0226	.687	2.737
2.598	.2296	.909	-.0242	.656	2.650
2.399	.2085	.838	-.0302	.597	2.488
2.242	.1963	.799	-.0275	.551	2.350
2.083	.1785	.758	-.0346	.491	2.206
1.900	.1729	.732	-.0289	.449	2.025
1.714	.1620	.711	-.0311	.390	1.834
1.563	.1540	.700	-.0270	.344	1.677
1.435	.1540	.703	-.0195	.314	1.538
1.259	.1537	.699	-.0205	.277	1.351
1.096	.1565	.707	-.0218	.243	1.174

TABLE NO. 29

Test No. 53

V/nD	C <sub>T</sub>	C <sub>P</sub>	$\Delta C_P$	$\eta$	C <sub>S</sub>
4.127	0.1959	1.018	0.0547	0.794	4.119
3.950	.2156	1.048	.0445	.812	3.914
3.810	.2310	1.070	.0374	.822	3.764
3.623	.2485	1.085	.0297	.830	3.569
3.430	.2617	1.082	.0074	.829	3.382
3.280	.2672	1.080	.0021	.810	3.237
3.138	.2699	1.062	-.0107	.796	3.107
2.968	.2606	1.020	-.0205	.773	2.962
2.790	.2475	.965	-.0222	.716	2.815
2.628	.2348	.913	-.0266	.676	2.678
2.447	.2218	.862	-.0233	.629	2.520
2.290	.2111	.826	-.0201	.585	2.382
2.130	.1847	.761	-.0351	.517	2.251
1.991	.1851	.752	-.0276	.490	2.110
1.815	.1732	.723	-.0300	.435	1.938
1.642	.1615	.709	-.0190	.374	1.759
1.500	.1566	.697	-.0179	.337	1.614
1.345	.1565	.696	-.0200	.303	1.447
1.205	.1572	.700	-.0147	.271	1.293
.985	.1581	.702	-.0169	.222	1.056

TABLE NO. 30

Four-Blade Dual Rotation Prop Small Spinner  
 $\beta_{RH} = 45^\circ$   $\beta_{LH} = 43.8^\circ$

Faired Blade Roots

Four-Blade Dual Rotation Prop Small Spinner  
 $\beta_{RH} = 65^\circ$   $\beta_{LH} = 62.5^\circ$

Faired Blade Roots

Test No. 40

V/nD	C <sub>T</sub>	C <sub>P</sub>	$\Delta C_P$	$\eta$	C <sub>S</sub>
2.349	0.0289	0.1281	+0.0108	0.530	3.545
2.253	.0590	.1823	+ .0080	.730	3.164
2.178	.0757	.2110	+ .0083	.781	2.973
2.070	.0996	.2467	+ .0055	.836	2.740
1.951	.1247	.2840	+ .0020	.857	2.513
1.865	.1446	.3130	+ .0007	.862	2.357
1.771	.1643	.3350	+ .0014	.869	2.210
1.682	.1790	.3500	- .0021	.860	2.076
1.589	.1895	.3630	- .0059	.830	1.950
1.486	.1985	.3730	- .0085	.791	1.813
1.396	.1999	.3730	- .0133	.748	1.704

Test No. 45

V/nD	C <sub>T</sub>	C <sub>P</sub>	$\Delta C_P$	$\eta$	C <sub>S</sub>
4.176	0.1943	1.032	0.0473	0.786	4.152
3.990	.2135	1.062	.0400	.802	3.950
3.837	.2307	1.090	.0346	.812	3.775
3.655	.2487	1.106	.0215	.822	3.545
3.464	.2621	1.109	.0108	.819	3.359
3.292	.2693	1.105	-.0011	.802	3.192
3.151	.2683	1.080	-.0119	.783	3.077
2.989	.2621	1.043	-.0194	.751	2.960
2.910	.2483	.985	-.0237	.708	2.819
2.685	.2325	.933	-.0334	.669	2.722
2.637	.2294	.920	-.0320	.658	2.684
2.457	.2129	.867	-.0287	.603	2.531
2.295	.1940	.812	-.0364	.548	2.390
2.152	.1829	.764	-.0352	.515	2.275

TABLE NO. 31

Three-Blade (E) Propeller  
 $\beta = 55^\circ$

Small Spinner  
Plain Blade Roots

Test No. 66

V/nD	$C_T$	$C_P$	$\eta$	$C_S$
1.654	0.0248	0.0662	0.820	2.845
1.578	.0418	.0863	.764	2.575
1.520	.0552	.1023	.820	2.401
1.438	.0702	.1185	.852	2.204
1.365	.0827	.1318	.857	2.050
1.311	.0913	.1390	.861	1.949
1.234	.1044	.1495	.862	1.805
1.162	.1142	.1577	.842	1.683
1.097	.1243	.1651	.826	1.571
1.027	.1320	.1710	.793	1.460
.950	.1345	.1773	.720	1.342
.888	.1358	.1777	.679	1.254
.816	.1366	.1791	.622	1.149
.760	.1380	.1820	.577	1.069
.689	.1404	.1836	.527	.967
.621	.1420	.1863	.473	.869
.564	.1444	.1897	.430	.786
.475	.1484	.1935	.364	.659
.409	.1508	.1973	.313	.565
1.625	.0331	.0744	.722	2.733
1.543	.0508	.0962	.816	2.465
1.484	.0633	.1103	.852	2.307
1.403	.0764	.1241	.863	2.132
1.336	.0886	.1365	.864	1.993
1.271	.0976	.1450	.856	1.873
1.202	.1100	.1541	.858	1.748
1.126	.1207	.1623	.938	1.619
1.065	.1285	.1671	.819	1.523
.990	.1360	.1733	.775	1.407
.918	.1363	.1780	.704	1.295
.862	.1365	.1784	.659	1.216

TABLE NO. 33

Three-Blade (E) Propeller  
 $\beta = 55^\circ$

Small Spinner  
Plain Blade Roots

Test No. 70

V/nD	$C_T$	$C_P$	$\eta$	$C_S$
2.990	0.0951	0.3455	0.823	3.703
2.847	.1098	.3731	.838	3.421
2.740	.1206	.3900	.848	3.306
2.615	.1320	.4095	.843	3.113
2.486	.1452	.4260	.848	2.946
2.374	.1524	.4390	.824	2.797
2.257	.1524	.4369	.787	2.663
2.136	.1519	.4310	.752	2.525
2.022	.1499	.4220	.717	2.402
1.911	.1471	.4122	.682	2.282
1.768	.1445	.4020	.636	2.126
1.651	.1430	.3975	.594	1.985
1.543	.1428	.3953	.557	1.859
1.424	.1417	.3930	.514	1.716
1.308	.1412	.3909	.472	1.579
1.192	.1411	.3925	.429	1.447
1.077	.1396	.3958	.380	1.296
.983	.1378	.3950	.343	1.182
.834	.1373	.3960	.289	1.002
.677	.1375	.3970	.234	.815
3.036	.0909	.3340	.826	3.787
2.935	.1009	.3570	.830	3.612
2.812	.1147	.3815	.847	3.408
2.658	.1278	.4017	.846	3.192
2.559	.1386	.4166	.851	3.045
2.437	.1475	.4285	.839	2.882
2.308	.1530	.4400	.803	2.720
2.189	.1522	.4330	.769	2.587
2.072	.1515	.4248	.739	2.457
1.949	.1480	.4140	.697	2.324

TABLE NO. 32

Three-Blade (E) Propeller  
 $\beta = 45^\circ$

Small Spinner  
Plain Blade Roots

Test No. 68

V/nD	$C_T$	$C_P$	$\eta$	$C_S$
2.313	0.0365	0.1226	0.688	3.514
2.234	.0496	.1465	.756	3.280
2.151	.0650	.1723	.812	3.050
2.050	.0789	.1913	.846	2.850
1.960	.0946	.2151	.862	2.660
1.859	.1090	.2340	.866	2.481
1.776	.1205	.2480	.864	2.363
1.687	.1324	.2603	.848	2.184
1.578	.1362	.2700	.797	2.048
1.482	.1374	.2697	.754	1.924
1.387	.1386	.2696	.713	1.803
1.297	.1391	.2706	.667	1.682
1.209	.1408	.2711	.627	1.566
1.114	.1415	.2720	.579	1.443
1.030	.1436	.2762	.535	1.333
.935	.1452	.2775	.490	1.197
.854	.1465	.2805	.446	1.100
.776	.1489	.2845	.407	.998
.663	.1516	.2911	.346	.843
.541	.1540	.2968	.281	.690
2.284	.0420	.1318	.729	3.421
2.190	.0593	.1614	.805	3.153
2.083	.0762	.1875	.846	2.910
1.994	.0892	.2071	.860	2.731
1.902	.1031	.2275	.864	2.560
1.801	.1158	.2416	.864	2.394
1.720	.1264	.2546	.856	2.261
1.625	.1347	.2662	.824	2.116
1.529	.1370	.2709	.775	1.986
1.456	.1380	.2709	.743	1.891
1.338	.1392	.2710	.695	1.747

TABLE NO. 34

Three-Blade (E) Propeller  
 $\beta = 65^\circ$

Small Spinner  
Plain Blade Roots

Test No. 73

V/nD	$C_T$	$C_P$	$\eta$	$C_S$
4.100	0.1516	0.7860	0.790	4.305
3.965	.1603	.7994	.796	4.151
3.815	.1730	.8140	.812	3.970
3.650	.1813	.8270	.800	3.797
3.466	.1877	.8220	.792	3.585
3.290	.1860	.8055	.759	3.436
3.121	.1801	.7700	.730	3.289
2.992	.1744	.7440	.701	3.176
2.788	.1636	.6920	.659	3.000
2.634	.1554	.6550	.625	2.869
2.490	.1487	.6250	.592	2.735
2.273	.1399	.5910	.538	2.523
2.120	.1340	.5669	.501	2.374
1.965	.1164	.5318	.430	2.228
1.803	.1118	.5179	.389	2.055
1.630	.1018	.4990	.333	1.872
1.491	.1014	.5000	.302	1.711
1.343	.0997	.4960	.270	1.543
1.138	.1042	.5000	.237	1.306
.988	.1044	.4990	.206	1.135
4.150	.1494	.7808	.789	4.358
4.020	.1577	.7940	.798	4.213
3.890	.1664	.8090	.800	4.055
3.710	.1775	.8190	.805	3.860
3.543	.1858	.8200	.803	3.685
3.372	.1883	.8160	.778	3.510
3.208	.1834	.7910	.743	3.363
3.050	.1780	.7585	.715	3.230
2.862	.1684	.7110	.678	3.062
2.742	.1613	.6820	.648	2.961

Three-Blade ( $E'$ ) Propeller  
 $\beta = 35^\circ$ Small Spinner  
Plain Blade RootsThree-Blade ( $E'$ ) Propeller  
 $\beta = 45^\circ$ Small Spinner  
Plain Blade Roots

Test No. 74				
$V/nD$	$C_T$	$C_P$	$\eta$	$C_S$
1.640	0.0353	0.0867	0.668	2.675
1.580	.0521	.1066	.772	2.476
1.502	.0705	.1290	.821	2.264
1.426	.0868	.1467	.838	2.096
1.353	.1012	.1624	.844	1.947
1.298	.1132	.1745	.843	1.841
1.229	.1273	.1874	.835	1.717
1.157	.1406	.1975	.816	1.600
1.091	.1520	.2079	.798	1.495
1.018	.1641	.2166	.772	1.382
.947	.1721	.2260	.722	1.275
.885	.1751	.2308	.672	1.186
.824	.1775	.2332	.627	1.103
.751	.1819	.2353	.580	1.003
.683	.1842	.2410	.522	.908
.617	.1888	.2432	.478	.819
.558	.1904	.2458	.433	.743
.475	.1988	.2509	.376	.627
.414	.2012	.2586	.321	.542
1.605	.0449	.0981	.734	2.553
1.532	.0629	.1206	.799	2.341
1.470	.0778	.1372	.834	2.188
1.391	.0948	.1553	.849	2.018
1.327	.1064	.1674	.843	1.898
1.258	.1211	.1815	.839	1.769
1.195	.1332	.1915	.832	1.661
1.116	.1474	.2032	.809	1.535
1.059	.1581	.2120	.790	1.445
.985	.1689	.2218	.750	1.330

Test No. 75				
$V/nD$	$C_T$	$C_P$	$\eta$	$C_S$
2.143	0.0835	0.2190	0.817	2.902
2.038	.1013	.2480	.831	2.690
1.950	.1181	.2726	.844	2.529
1.837	.1354	.2946	.844	2.348
1.760	.1490	.3121	.840	2.223
1.665	.1641	.3304	.827	2.081
1.576	.1726	.3438	.792	1.954
1.473	.1771	.3500	.745	1.819
1.390	.1788	.3520	.706	1.714
1.286	.1829	.3540	.664	1.583
1.199	.1846	.3560	.622	1.475
1.118	.1881	.3601	.584	1.373
1.020	.1919	.3650	.537	1.249
.944	.1965	.3710	.500	1.152
.844	.2010	.3765	.451	1.028
.770	.2028	.3797	.412	.934
.657	.2070	.3868	.352	.794
.543	.2100	.3950	.289	.653
2.320	.0472	.1601	.684	3.343
2.229	.0662	.1917	.770	3.098
2.272	.0567	.1744	.749	3.224
2.188	.0770	.2089	.806	2.993
2.081	.0933	.2359	.824	2.778
1.998	.1108	.2604	.850	2.617
1.894	.1262	.2816	.848	2.443
1.805	.1418	.3034	.843	2.292
1.717	.1554	.3208	.832	2.160
1.625	.1670	.3340	.812	2.026
1.526	.1753	.3503	.763	1.884

TABLE NO. 37

TABLE NO. 38

Three-Blade ( $E'$ ) Propeller  
 $\beta = 55^\circ$ Small Spinner  
Plain Blade RootsThree-Blade ( $E'$ ) Propeller  
 $\beta = 65^\circ$ Small Spinner  
Plain Blade Roots

Test No. 76				
$V/nD$	$C_T$	$C_P$	$\eta$	$C_S$
2.974	0.1216	0.4367	0.829	3.509
2.860	.1325	.4640	.817	3.329
2.753	.1463	.4892	.824	3.169
2.625	.1615	.5115	.829	2.995
2.494	.1768	.5343	.826	2.828
2.376	.1882	.5530	.809	2.675
2.265	.1915	.5600	.775	2.546
2.142	.1930	.5575	.742	2.410
2.017	.1922	.5491	.707	2.275
1.900	.1913	.5415	.671	2.147
1.772	.1916	.5342	.636	2.008
1.646	.1916	.5289	.597	1.868
1.539	.1915	.5270	.559	1.747
1.421	.1927	.5260	.521	1.614
1.312	.1934	.5278	.481	1.489
1.197	.1950	.5305	.440	1.357
1.075	.1969	.5370	.394	1.217
.990	.1977	.5410	.362	1.119
.841	.1978	.5405	.308	.950
.732	.1978	.5410	.268	.827
3.028	.1112	.4212	.799	3.600
2.900	.1265	.4560	.804	3.390
2.800	.1406	.4760	.828	3.242
2.665	.1562	.5059	.823	3.051
2.550	.1700	.5262	.824	2.899
2.427	.1839	.5480	.814	2.738
2.310	.1903	.5580	.788	2.596
2.203	.1925	.5611	.757	2.472
2.082	.1927	.5535	.725	2.344
1.946	.1914	.5450	.683	2.199

Test No. 77				
$V/nD$	$C_T$	$C_P$	$\eta$	$C_S$
4.115	0.1811	0.9668	0.771	4.148
3.943	.1921	.9870	.768	3.951
3.810	.2032	1.0020	.774	3.810
3.623	.2165	1.0120	.775	3.619
3.463	.2280	1.0200	.774	3.456
3.280	.2307	1.0180	.746	3.267
3.100	.2240	.9810	.708	3.106
2.950	.2163	.9356	.682	2.988
2.791	.2075	.8900	.651	2.855
2.618	.2002	.8500	.617	2.697
2.441	.1935	.8160	.579	2.541
2.274	.1882	.7890	.542	2.385
2.122	.1811	.7590	.506	2.247
1.950	.1696	.7280	.454	2.080
1.811	.1650	.7110	.421	1.940
1.644	.1620	.7030	.379	1.764
1.510	.1608	.6970	.348	1.623
1.343	.1611	.6910	.313	1.448
1.139	.1616	.6880	.268	1.229
.976	.1600	.6800	.230	1.054
4.181	.1778	.9678	.767	4.210
4.030	.1875	.9800	.771	4.046
3.870	.1986	.9940	.773	3.874
3.675	.2133	1.0130	.774	3.671
3.530	.2238	1.0190	.776	3.519
3.370	.2320	1.0210	.766	3.360
3.196	.2281	1.0000	.730	3.196
3.039	.2218	.9630	.700	3.066
2.865	.2123	.9150	.665	2.917
2.697	.2035	.8690	.631	2.778

TABLE NO. 39

TABLE NO. 40 Tables 39, 40, 41, 42

Two-Blade ( $E^H$ ) Propeller  
 $\beta = 35^\circ$ Small Spinner  
Plain Blade RootsTwo-Blade ( $E^H$ ) Propeller  
 $\beta = 45^\circ$ Small Spinner  
Plain Blade Roots

Test No. 67

$V/nD$	$C_T$	$C_P$	$\eta$	$C_S$
1.638	0.0225	0.0568	0.649	2.904
1.579	0.0333	0.0700	0.758	2.690
1.507	0.0466	0.0860	0.816	2.461
1.427	0.0608	0.1031	0.841	2.250
1.354	0.0732	0.1158	0.856	2.084
1.298	0.0816	0.1239	0.856	1.973
1.227	0.0928	0.1350	0.843	1.833
1.160	0.1023	0.1428	0.832	1.715
1.089	0.1145	0.1521	0.819	1.588
1.022	0.1233	0.1576	0.800	1.480
0.948	0.1333	0.1628	0.776	1.363
0.886	0.1370	0.1734	0.700	1.258
0.817	0.1394	0.1769	0.644	1.154
0.754	0.1413	0.1795	0.597	1.064
0.684	0.1452	0.1815	0.547	0.960
0.620	0.1500	0.1858	0.500	0.867
0.562	0.1520	0.1893	0.451	0.783
0.496	0.1568	0.1951	0.399	0.688
0.410	0.1606	0.2005	0.328	0.565
0.318	0.0264	0.0616	0.693	2.824
1.532	0.0421	0.0802	0.804	2.536
1.465	0.0535	0.0937	0.837	2.353
1.401	0.0660	0.1074	0.861	2.179
1.327	0.0762	0.1186	0.852	2.033
1.260	0.0876	0.1295	0.852	1.899
1.192	0.0991	0.1394	0.847	1.770
1.121	0.1093	0.1482	0.826	1.645
1.058	0.1186	0.1544	0.813	1.536
0.984	0.1298	0.1608	0.794	1.417
0.915	0.1368	0.1634	0.766	1.315

Test No. 69

$V/nD$	$C_T$	$C_P$	$\eta$	$C_S$
2.340	0.0237	0.0964	0.576	3.734
2.240	0.0415	0.1272	0.731	3.384
2.169	0.0532	0.1443	0.805	3.200
2.057	0.0692	0.1703	0.836	2.931
1.955	0.0822	0.1904	0.844	2.721
1.855	0.0958	0.2088	0.851	2.539
1.762	0.1084	0.2248	0.850	2.376
1.675	0.1183	0.2370	0.836	2.233
1.600	0.1276	0.2455	0.832	2.117
1.503	0.1362	0.2555	0.801	1.973
1.379	0.1399	0.2650	0.728	1.799
1.299	0.1405	0.2678	0.681	1.691
1.207	0.1419	0.2679	0.639	1.571
1.121	0.1454	0.2708	0.602	1.457
1.018	0.1494	0.2766	0.550	1.316
0.929	0.1522	0.2826	0.503	1.196
0.844	0.1569	0.2871	0.461	1.083
0.756	0.1607	0.2908	0.419	0.968
0.672	0.1639	0.2965	0.372	0.858
0.557	0.1699	0.3042	0.309	0.707
2.286	0.0347	0.1149	0.690	3.525
2.217	0.0459	0.1336	0.761	3.319
2.097	0.0626	0.1622	0.809	3.037
2.010	0.0754	0.1793	0.846	2.834
1.898	0.0902	0.2005	0.854	2.617
1.805	0.1026	0.2178	0.850	2.449
1.720	0.1131	0.2301	0.846	2.305
1.637	0.1238	0.2421	0.837	2.177
1.527	0.1352	0.2521	0.819	2.012
1.445	0.1378	0.2631	0.757	1.893
1.346	0.1409	0.2672	0.709	1.754

TABLE NO. 41

TABLE NO. 42

Two-Blade ( $E^H$ ) Propeller  
 $\beta = 55^\circ$ Small Spinner  
Plain Blade RootsTwo-Blade ( $E^H$ ) Propeller  
 $\beta = 65^\circ$ Small Spinner  
Plain Blade Roots

Test No. 71

$V/nD$	$C_T$	$C_P$	$\eta$	$C_S$
2.982	0.0802	0.2952	0.810	3.808
2.872	0.0929	0.3220	0.829	3.604
2.748	0.1071	0.3430	0.858	3.408
2.620	0.1161	0.3645	0.834	3.210
2.495	0.1297	0.3833	0.844	3.019
2.370	0.1407	0.3988	0.836	2.846
2.270	0.1485	0.4100	0.822	2.715
2.144	0.1497	0.4185	0.767	2.551
2.005	0.1471	0.4100	0.719	2.398
1.883	0.1460	0.4039	0.679	2.260
1.777	0.1470	0.3981	0.656	2.136
1.652	0.1464	0.3970	0.609	1.986
1.537	0.1471	0.3972	0.569	1.847
1.422	0.1480	0.3992	0.527	1.708
1.311	0.1494	0.4000	0.489	1.575
1.202	0.1512	0.4031	0.451	1.442
1.083	0.1543	0.4060	0.412	1.300
0.962	0.1556	0.4096	0.366	1.151
0.848	0.1563	0.4120	0.322	1.013
0.718	0.1567	0.4120	0.273	0.858
3.010	0.0787	0.2919	0.812	3.853
2.920	0.0863	0.3069	0.822	3.706
2.796	0.0997	0.3344	0.833	3.487
2.661	0.1128	0.3571	0.848	3.273
2.553	0.1229	0.3760	0.834	3.107
2.425	0.1349	0.3920	0.834	2.925
2.314	0.1445	0.4052	0.825	2.777
2.195	0.1500	0.4158	0.792	2.614
2.071	0.1487	0.4143	0.743	2.469
1.946	0.1474	0.4080	0.703	2.331
1.846	0.1468	0.4035	0.672	2.215

Test No. 72

$V/nD$	$C_T$	$C_P$	$\eta$	$C_S$
4.105	0.1292	0.6925	0.768	4.121
3.940	0.1385	0.7085	0.770	4.220
3.780	0.1486	0.7210	0.780	4.045
3.611	0.1580	0.7315	0.781	3.849
3.430	0.1694	0.7390	0.786	3.650
3.255	0.1761	0.7370	0.777	3.463
3.090	0.1748	0.7329	0.737	3.291
2.970	0.1692	0.7155	0.702	3.178
2.803	0.1605	0.6720	0.670	3.033
2.601	0.1516	0.6330	0.623	2.848
2.468	0.1470	0.6105	0.594	2.722
2.280	0.1413	0.5850	0.551	2.538
2.159	0.1383	0.5715	0.522	2.418
1.975	0.1349	0.5580	0.477	2.220
1.810	0.1316	0.5430	0.439	2.045
1.635	0.1271	0.5340	0.389	1.853
1.500	0.1256	0.5290	0.356	1.701
1.355	0.1247	0.5235	0.322	1.541
1.199	0.1255	0.5200	0.289	1.367
0.980	0.1238	0.5185	0.234	1.117
4.151	0.1252	0.6870	0.756	4.479
4.040	0.1323	0.6965	0.768	4.343
3.860	0.1440	0.7120	0.781	4.130
3.700	0.1530	0.7230	0.782	3.952
3.539	0.1645	0.7391	0.788	3.762
3.362	0.1740	0.7438	0.787	3.567
3.190	0.1783	0.7371	0.774	3.391
3.032	0.1744	0.7289	0.726	3.235
2.865	0.1645	0.6910	0.682	3.086
2.693	0.1555	0.6480	0.647	2.935



Figure 1.-Six-blade propeller with small spinner. (Filletted blade roots)

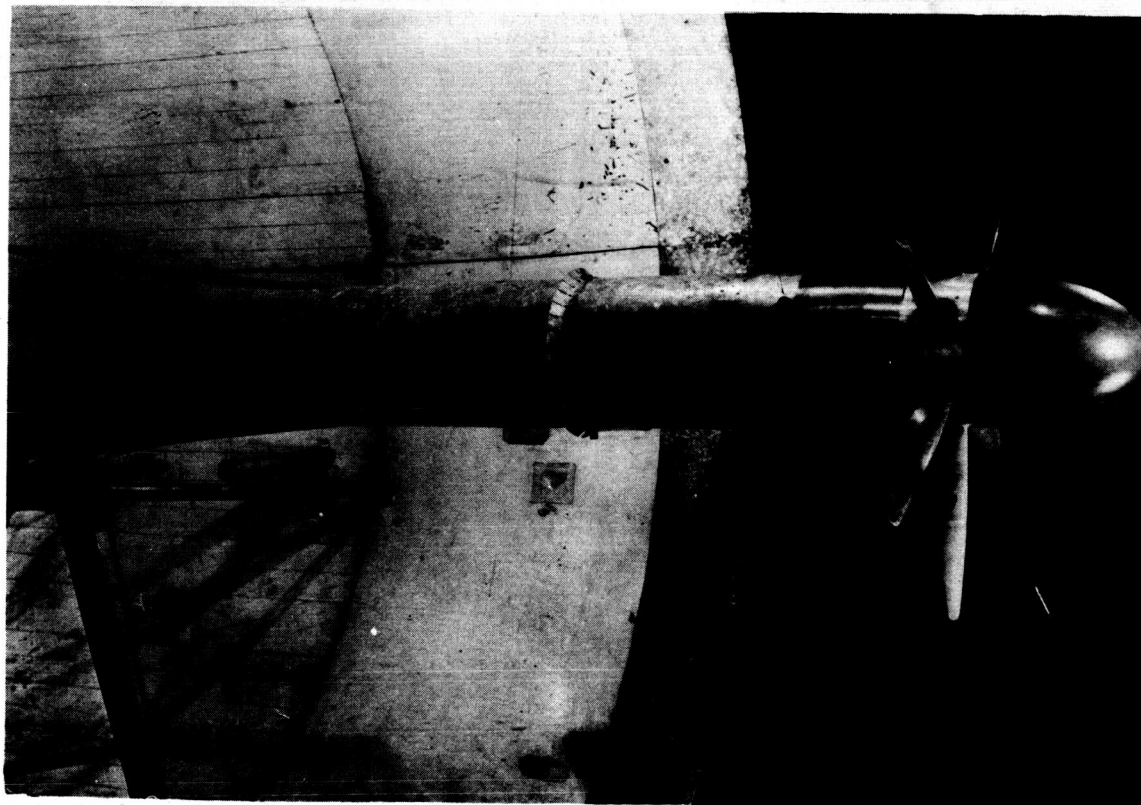


Figure 2.- Six-blade propeller with large spinner. (Apertures closed)

W-84

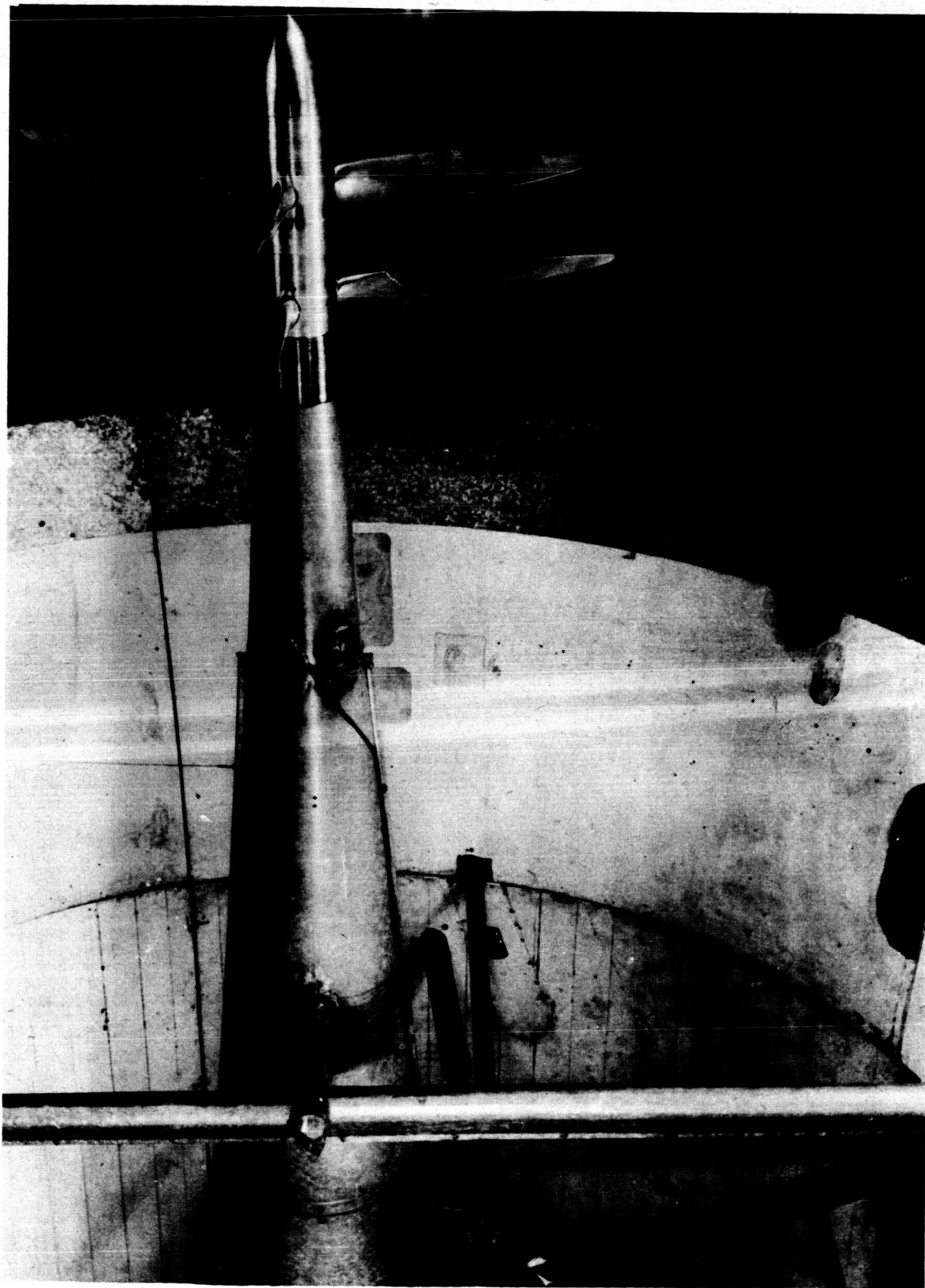


Figure 3.- Six-blade dual-rotation propeller with small spinner.

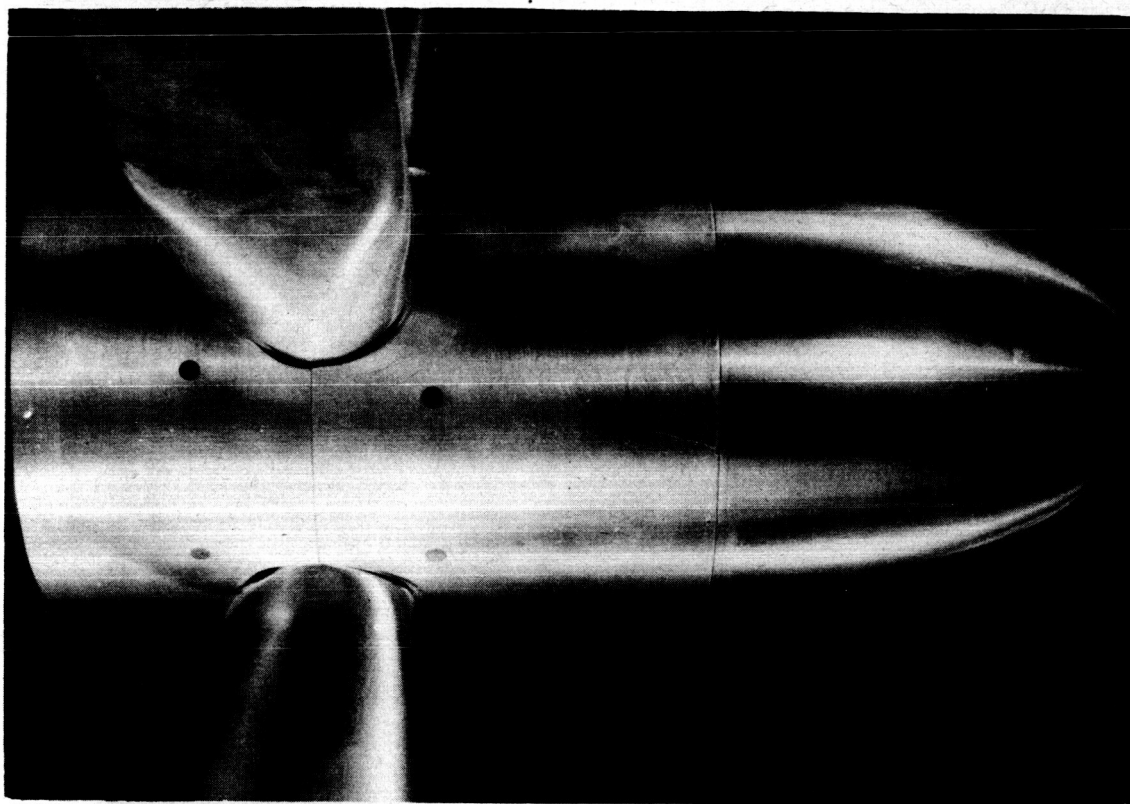


Figure 4.- Small spinner - plain blade roots.

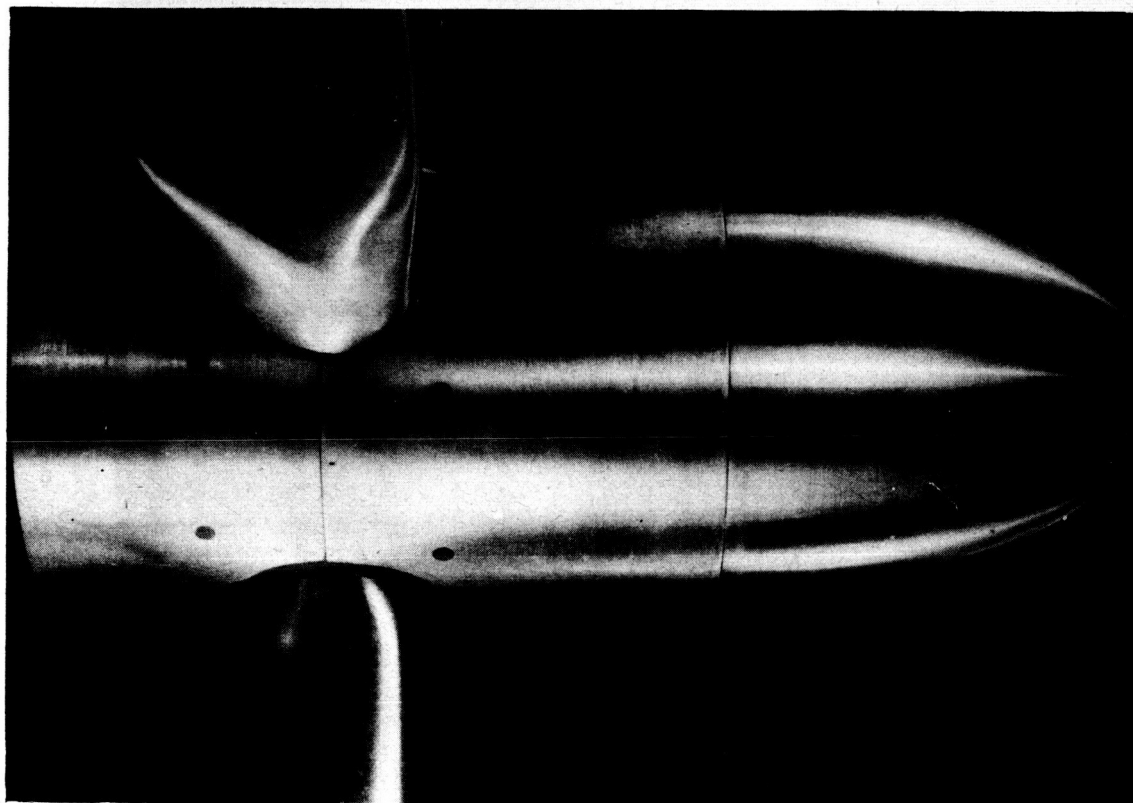


Figure 5.- Small spinner - filleted blade roots.

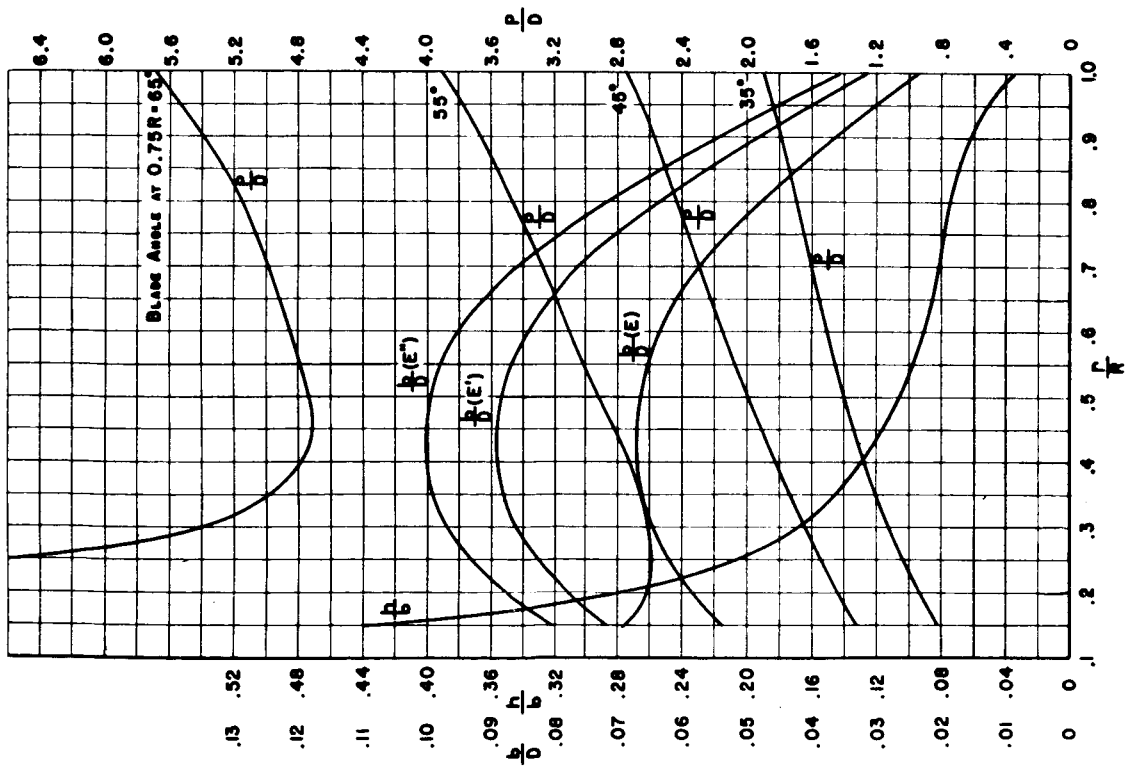


Figure 6.- Blade form curves.

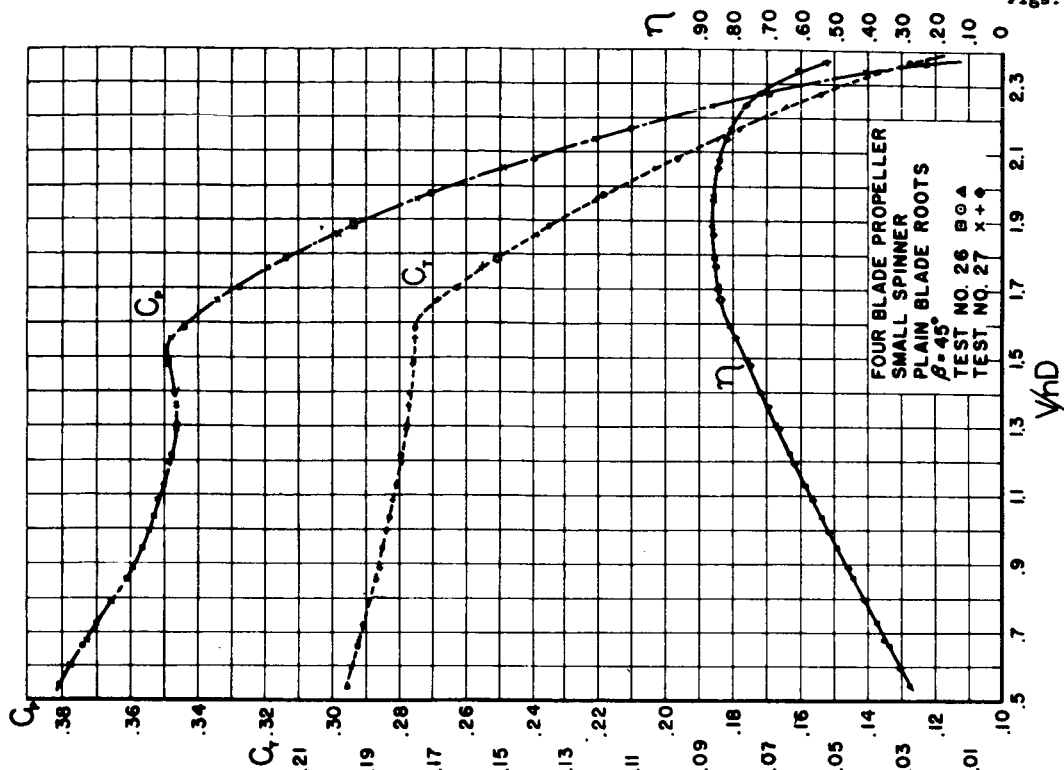


Figure 7.- Typical test results.

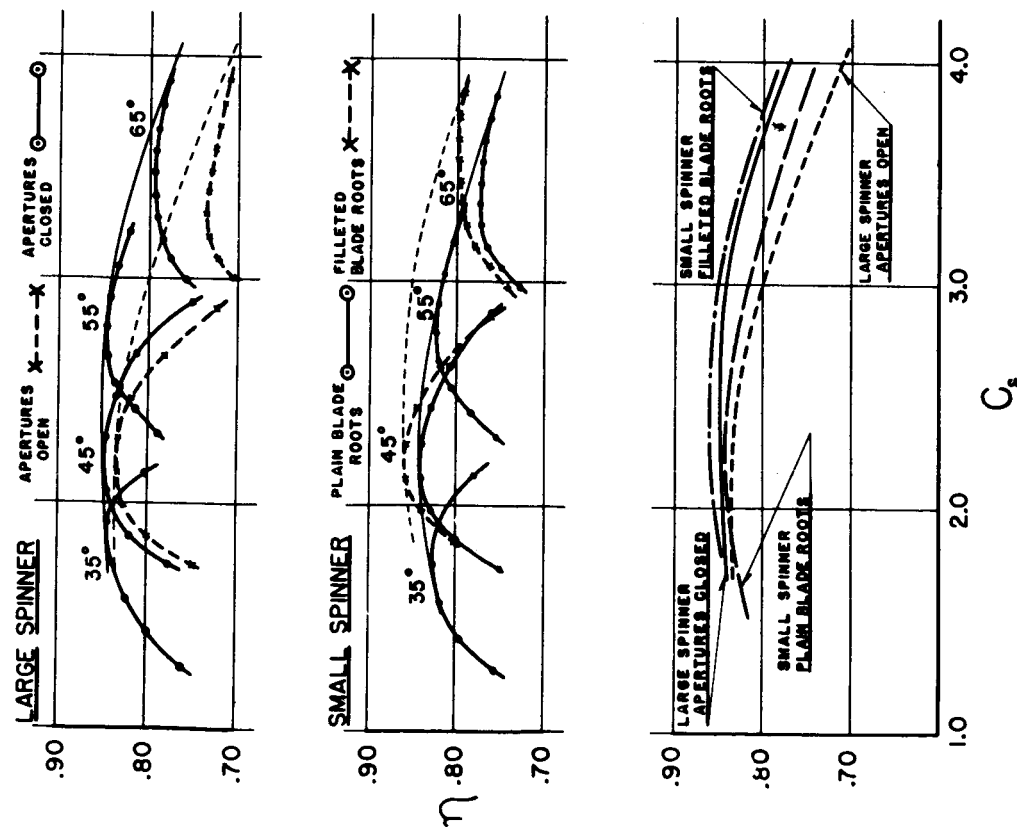


Figure 8.- Six-blade single-rotation propellers with spinners of 0.118 D and 0.278 D.

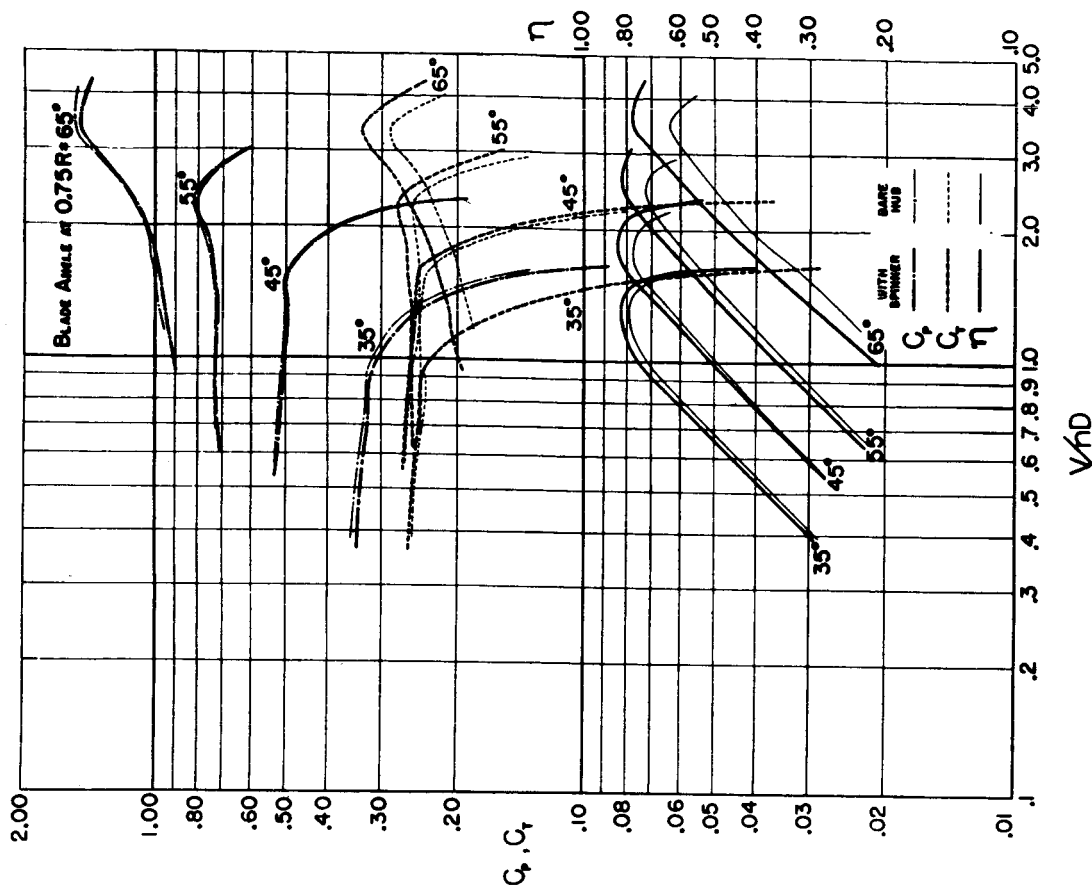
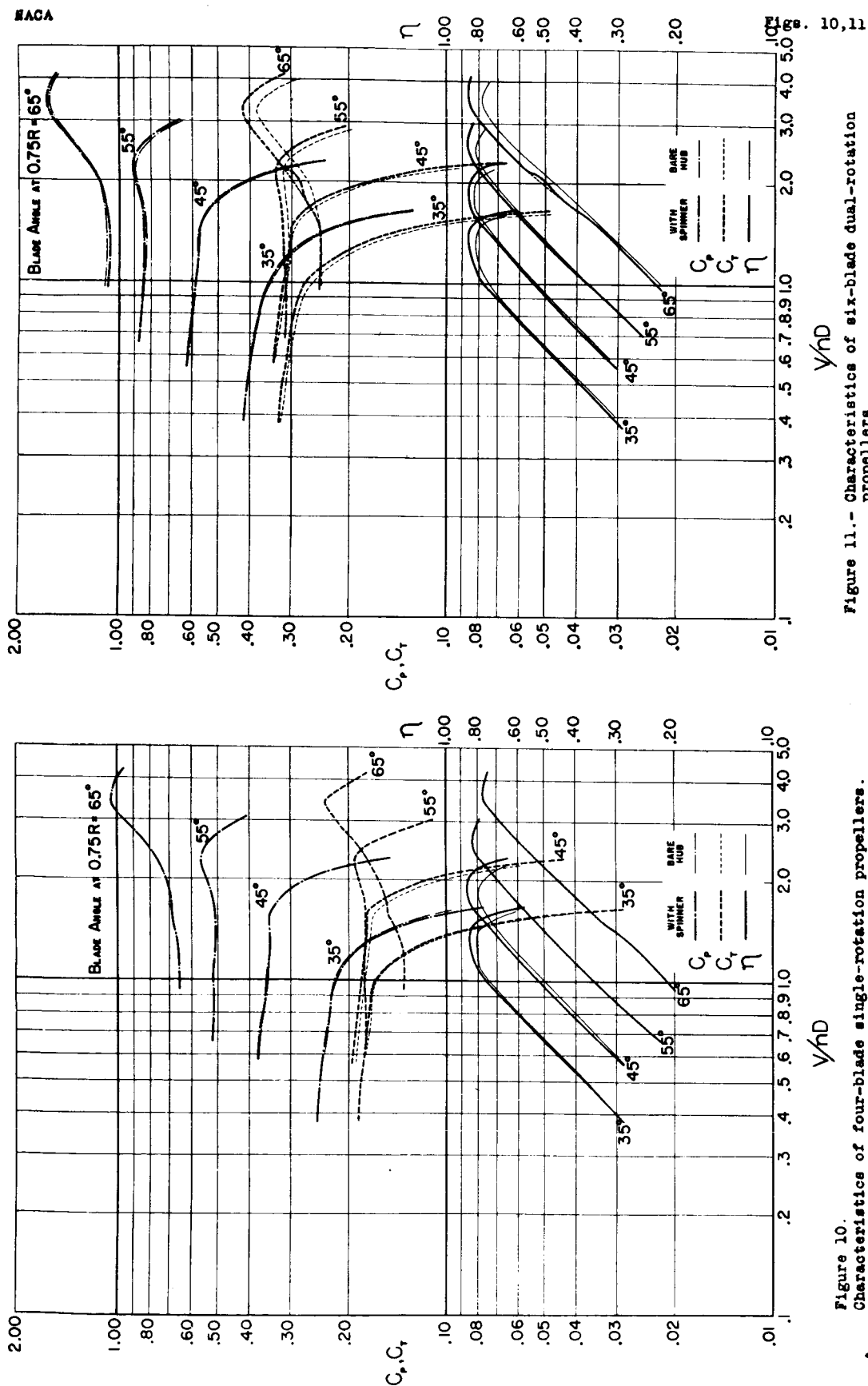


Figure 9.- Characteristics of six-blade single-rotation propellers.



NACA

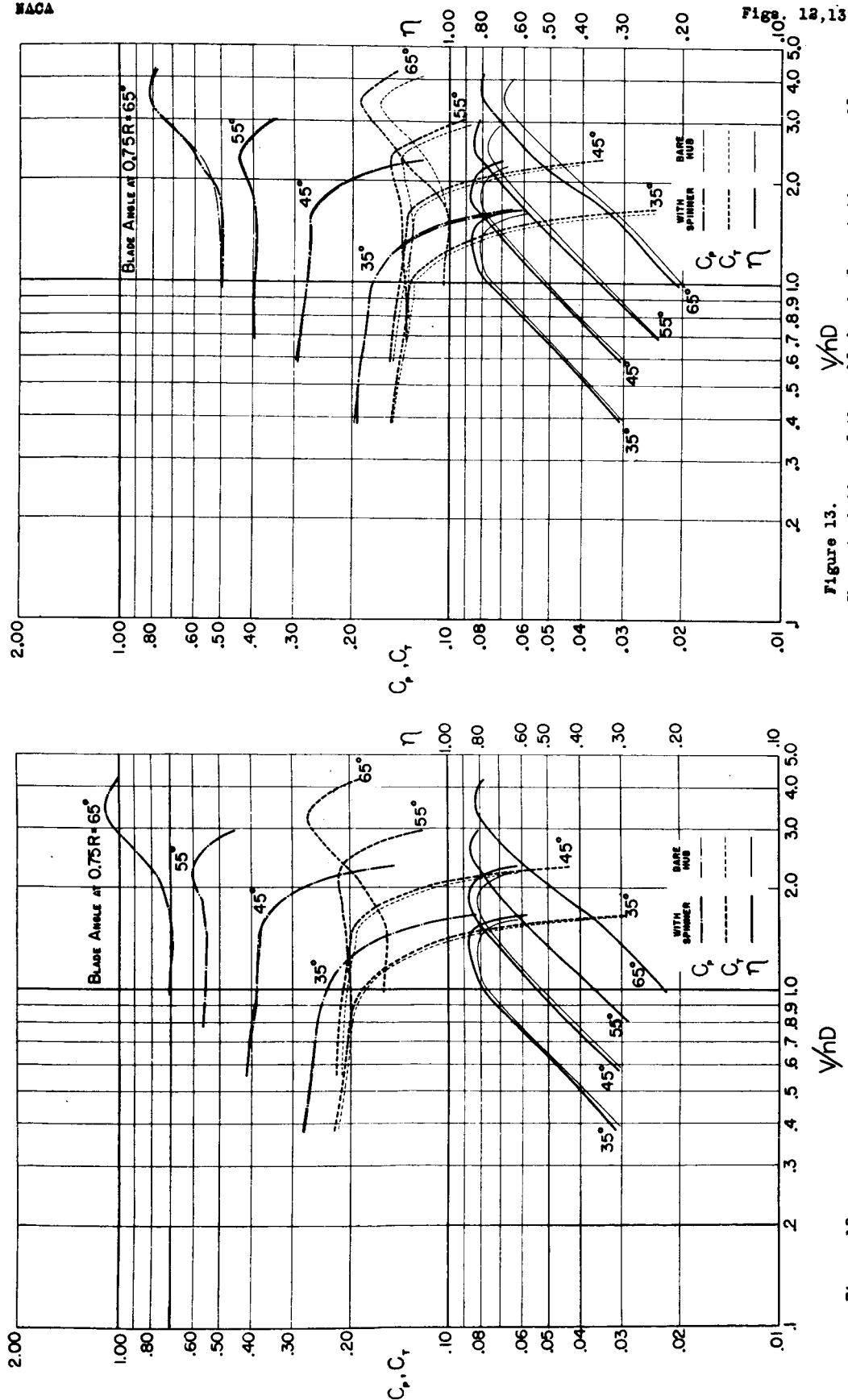


Figure 12.  
Characteristics of four-blade dual-rotation propellers.

Figure 13.  
Characteristics of three-blade single-rotation propellers.

NACA

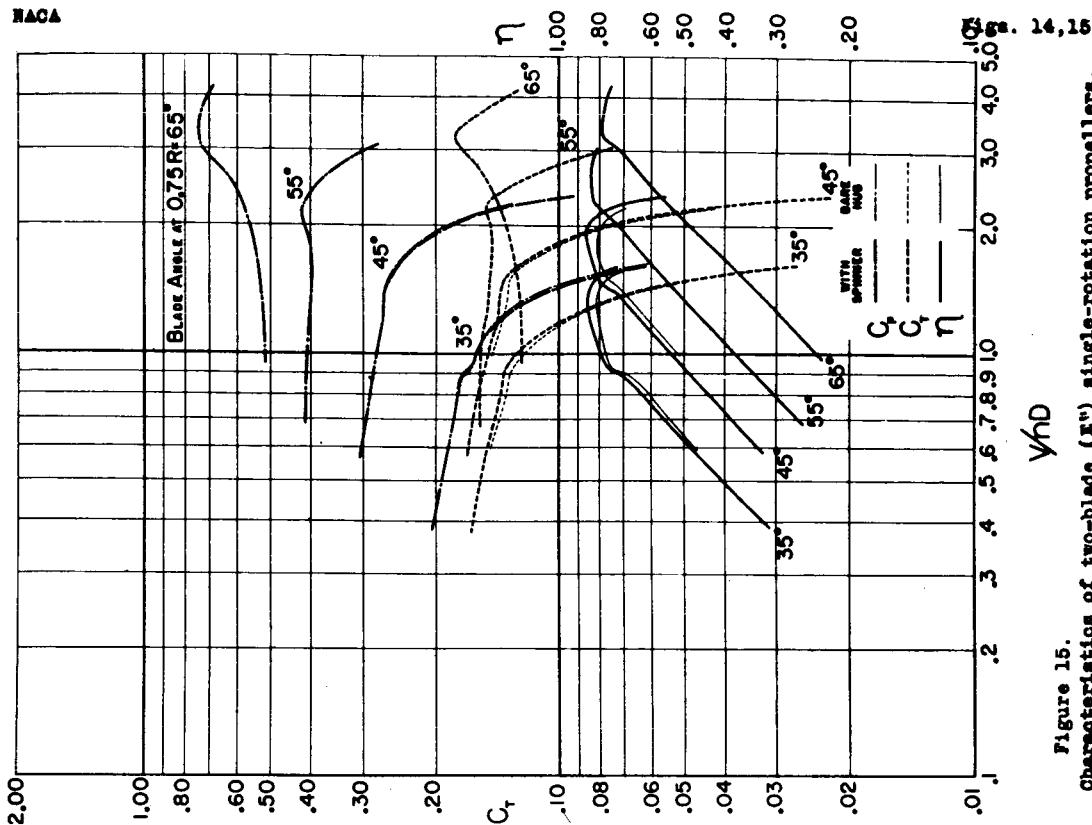


Figure 14.  
Characteristics of three-blade (21) single-rotation propellers.

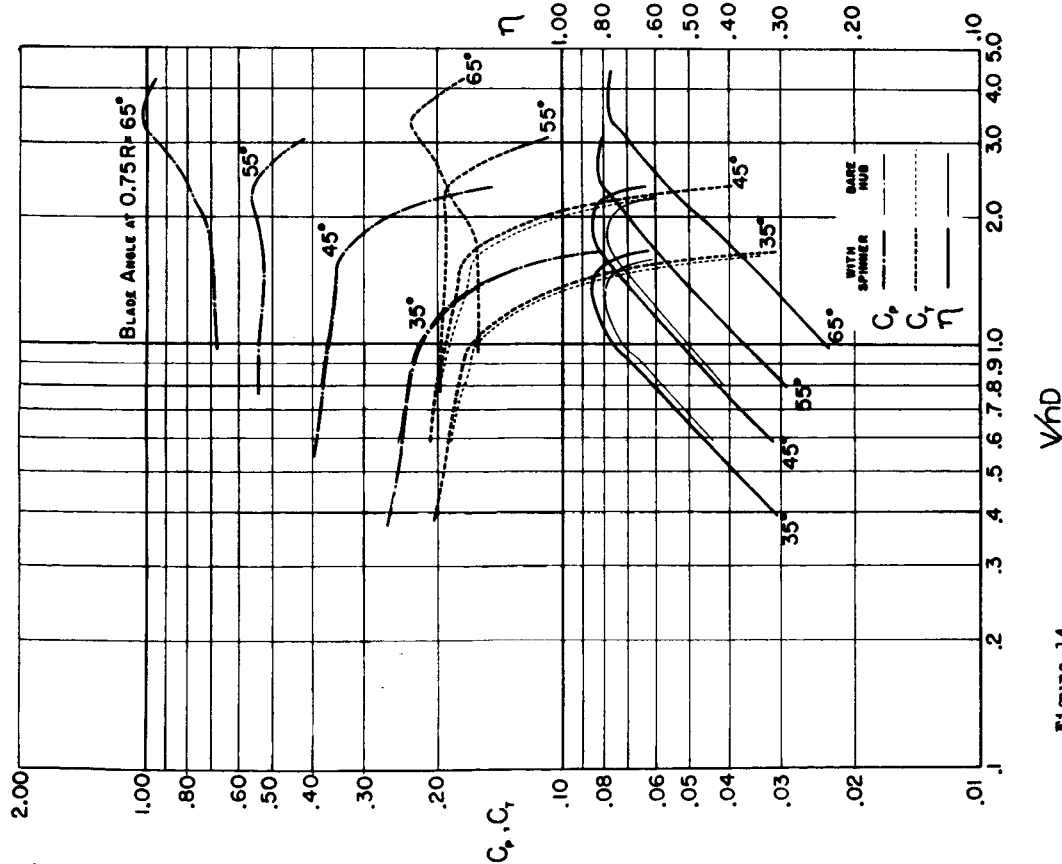


Figure 15.  
Characteristics of two-blade (21) single-rotation propellers.

SIX BLADE - DUAL ROTATION  
 FOUR BLADE - " "  
 SIX BLADE - SINGLE ROTATION  
 FOUR BLADE - " "  
 THREE BLADE - " "

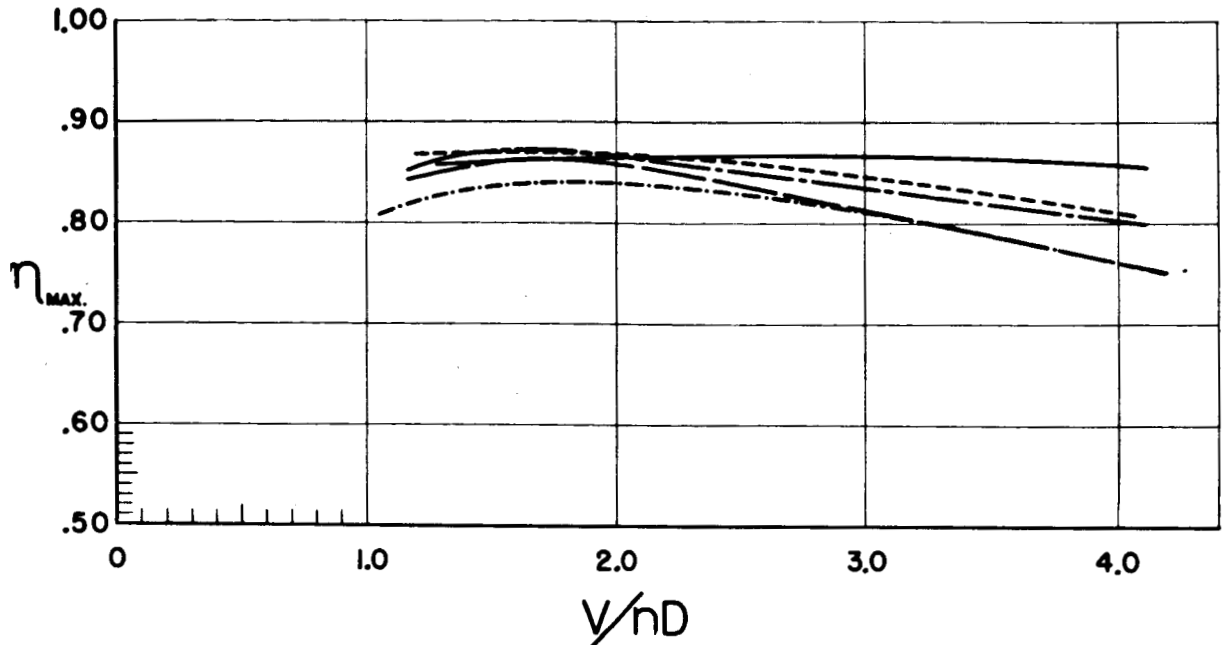


Figure 17.- Envelope efficiency curves for propellers with E-type blades and small spinners.

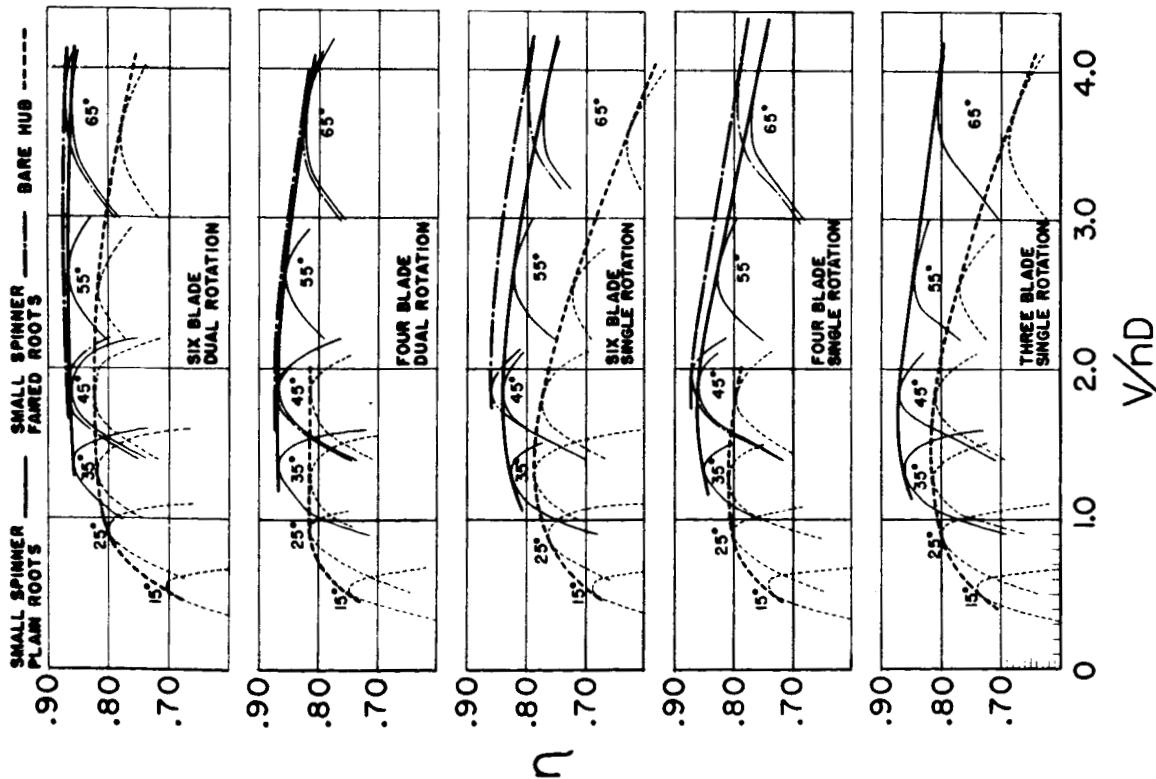


Figure 16.- Effects of spinners on efficiency of propellers with E-type blades.

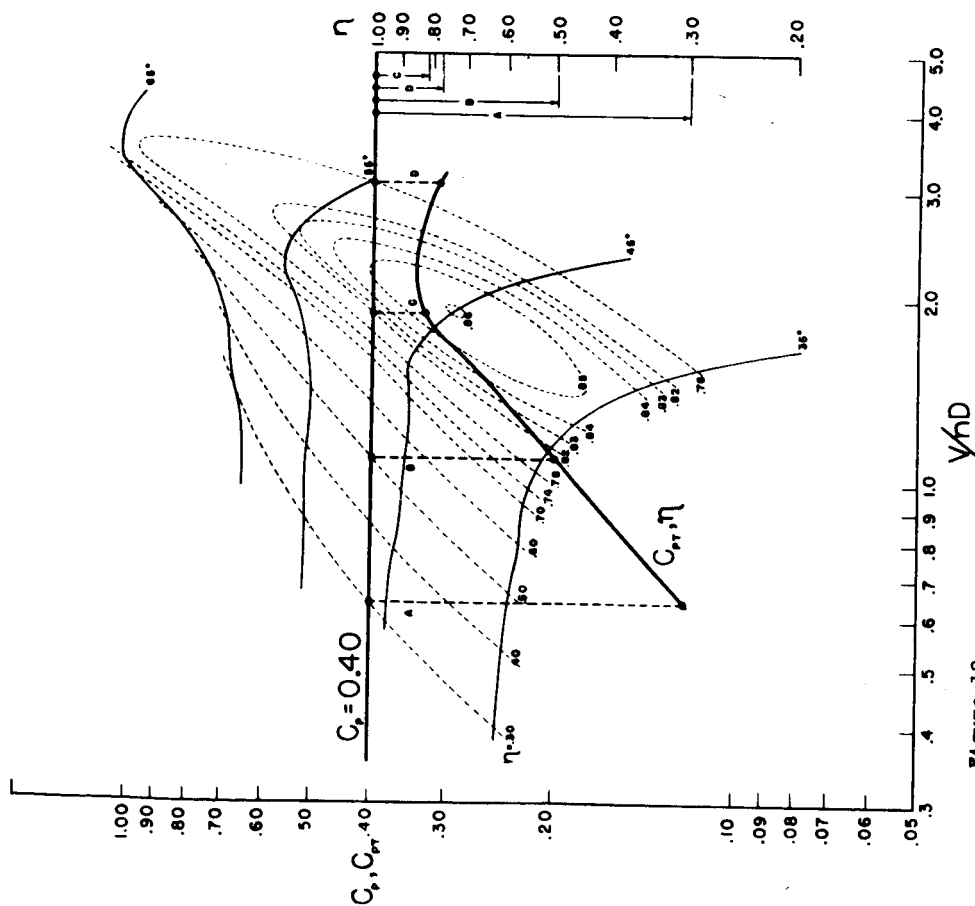


Figure 18.  
Construction of  $\eta$  (or  $C_{PT}$ ) vs.  $V/nD$  curve for  
constant-speed propeller operating at  $C_p = 0.40$ .

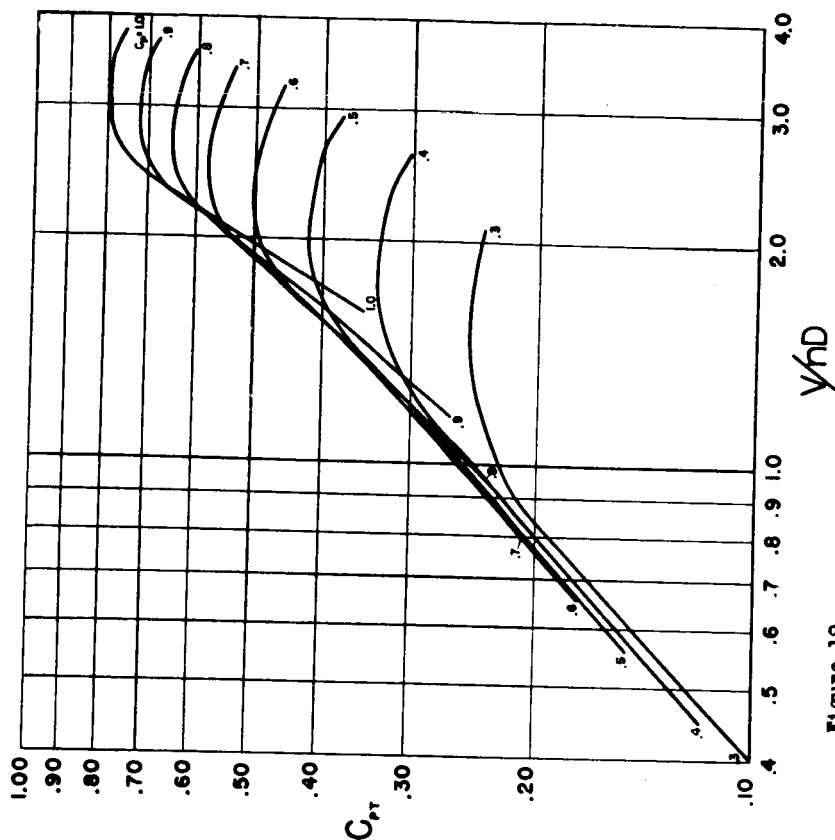


Figure 19.  
Characteristics of six-blade, single-rotation,  
constant-speed propellers with small spinners.

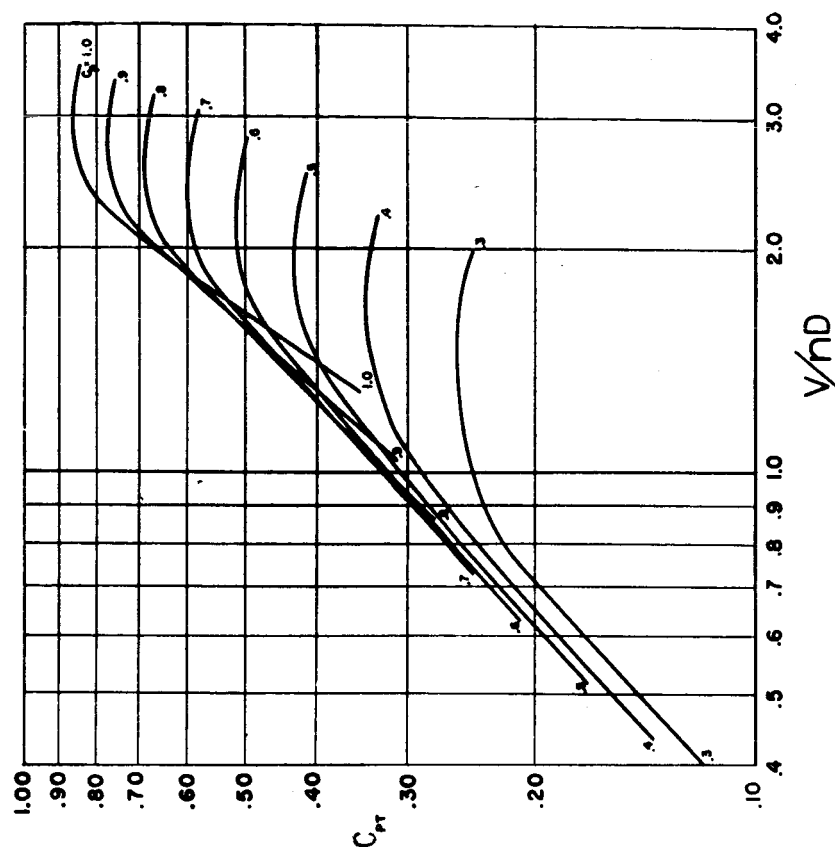


Figure 21.- Characteristics of six-blade, dual-rotation, constant-speed propellers with small spinner.

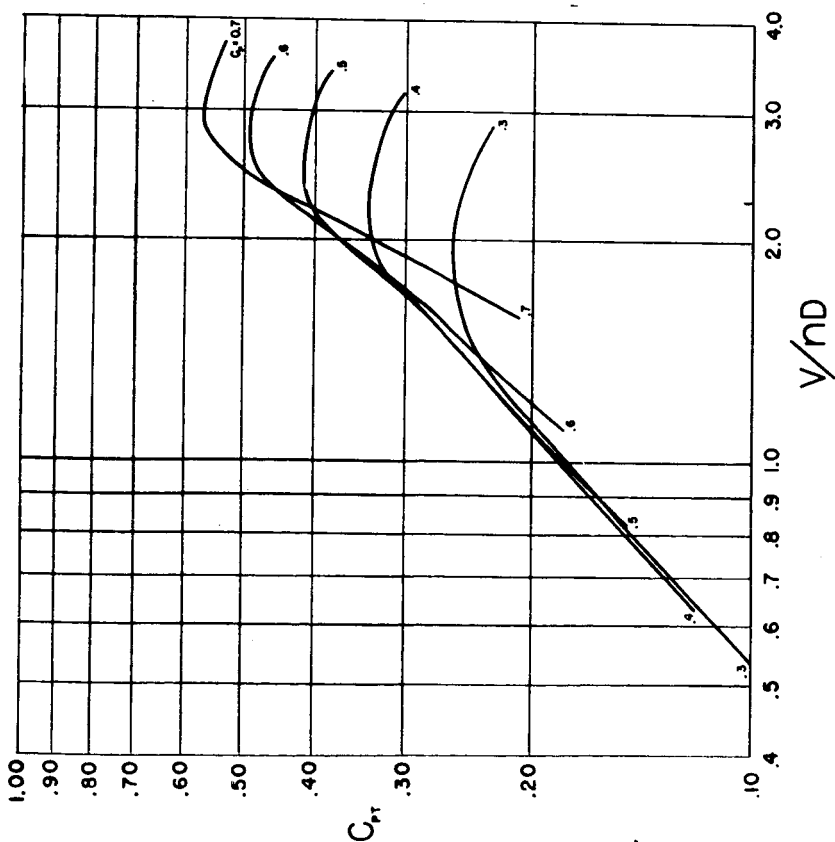


Figure 20.- Characteristics of four-blade, single-rotation, constant-speed propellers with small spinner.

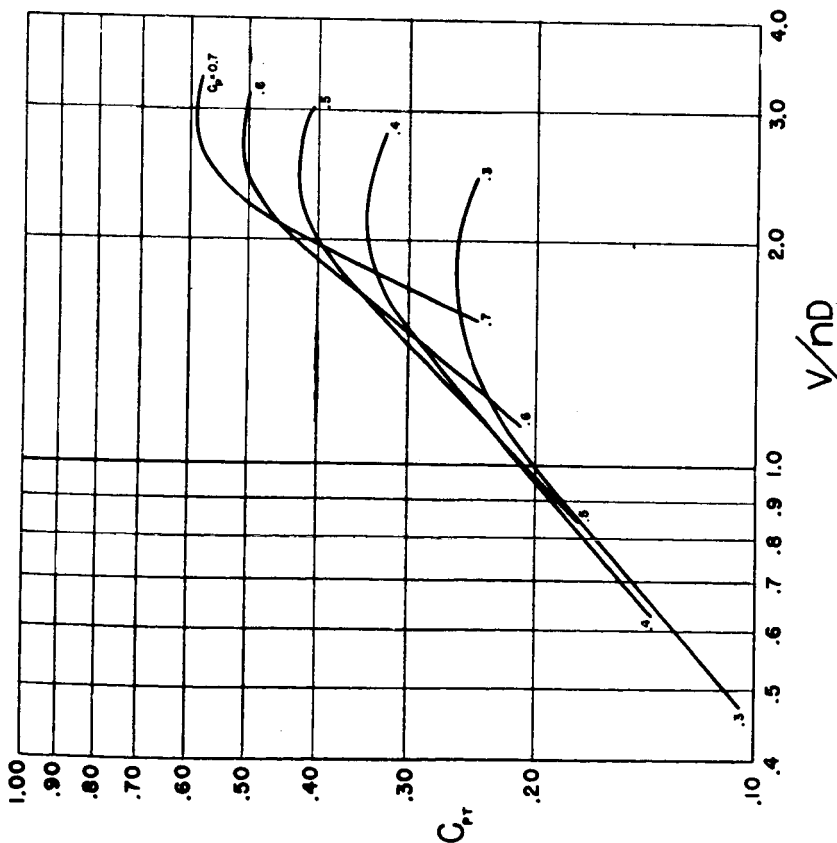


Figure 22.- Characteristics of four-blade, dual-rotation, constant-speed propellers with small spinners.

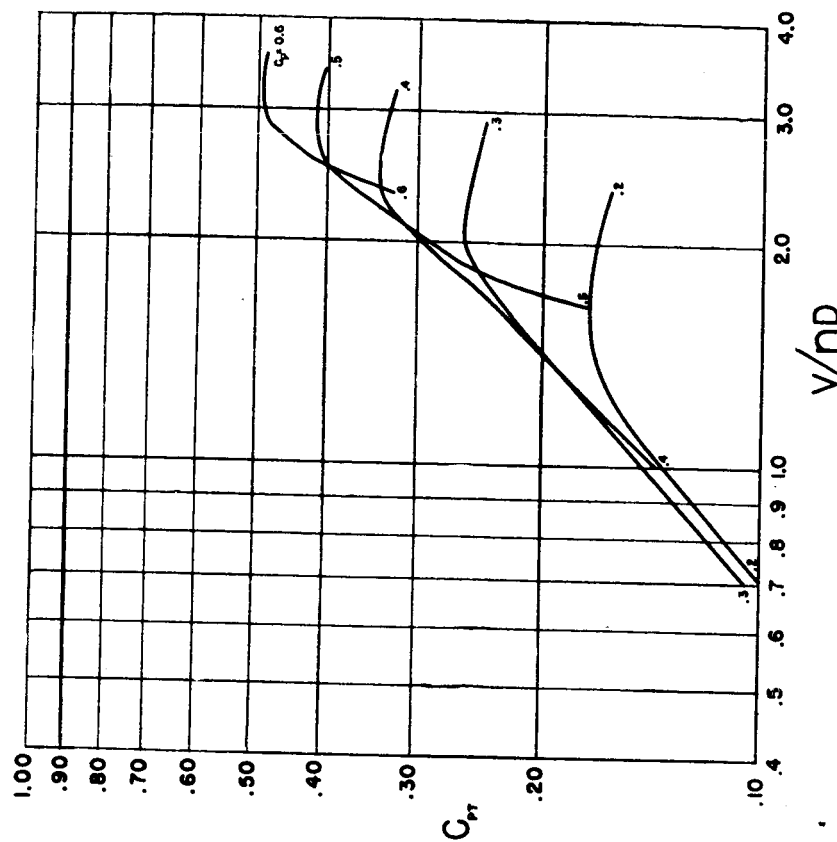


Figure 23.- Characteristics of three-blade, single-rotation, constant-speed propellers with small spinners.

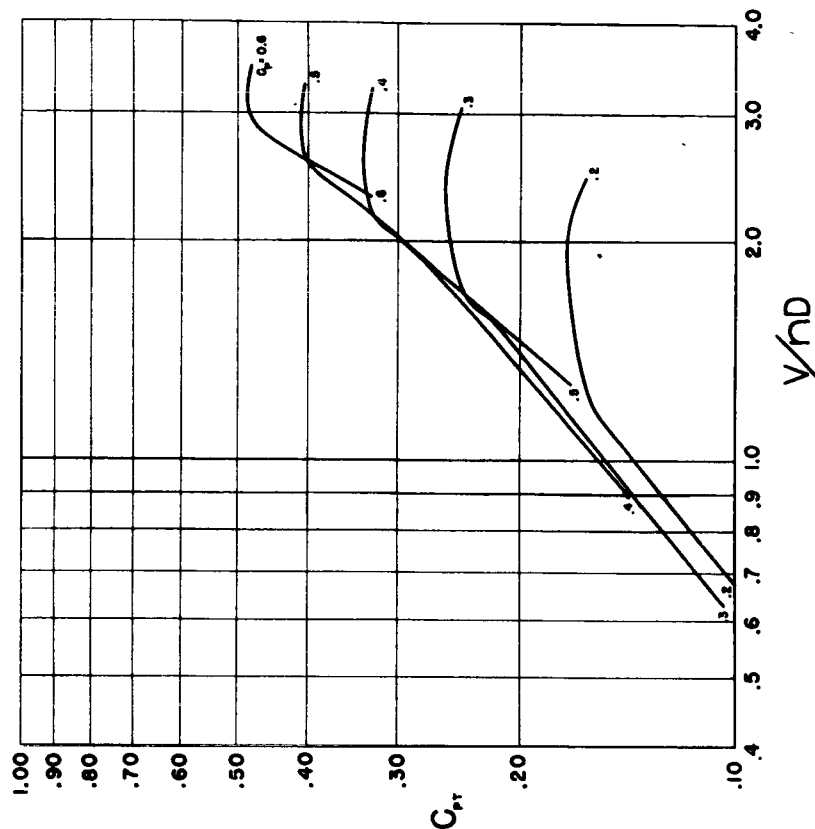


Figure 25.- Characteristics of two-blade ( $E''$ ), single-rotation, constant-speed propellers with small spinners.

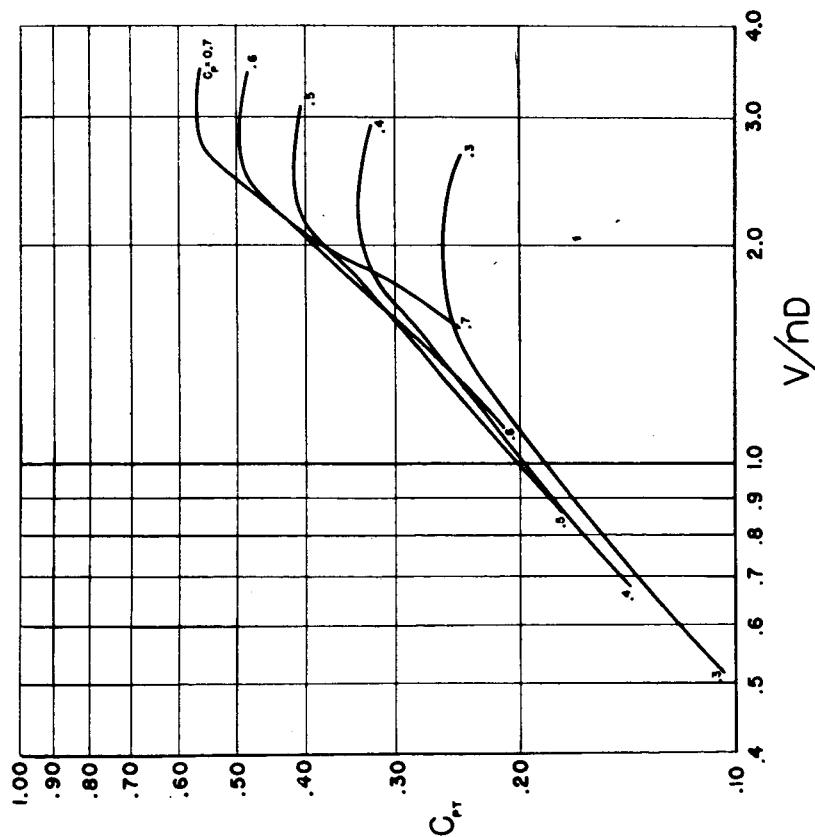


Figure 24.- Characteristics of three-blade ( $E'$ ), single-rotation, constant-speed propellers with small spinners.

NACA

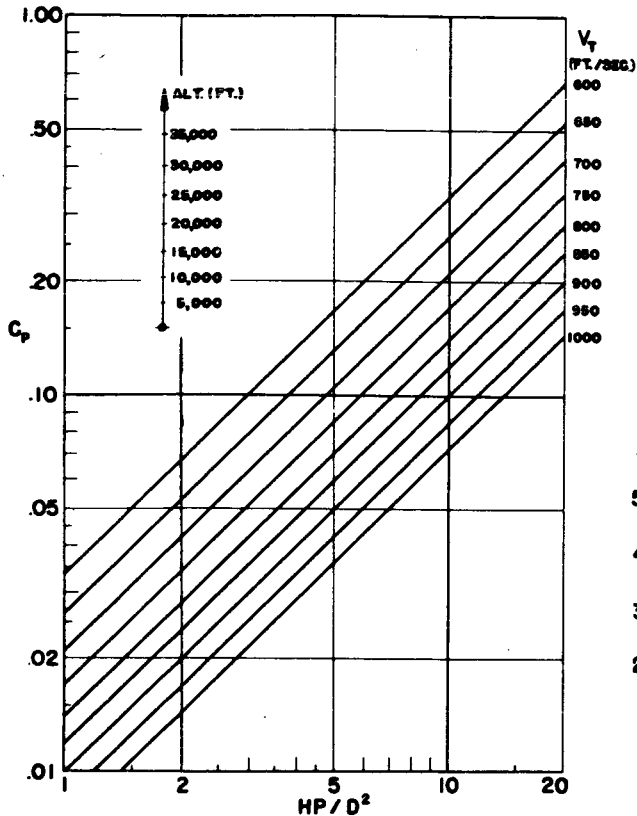


Figure 28.- Chart for evaluation of  $C_p$ .

Figs. 26,27,28,29

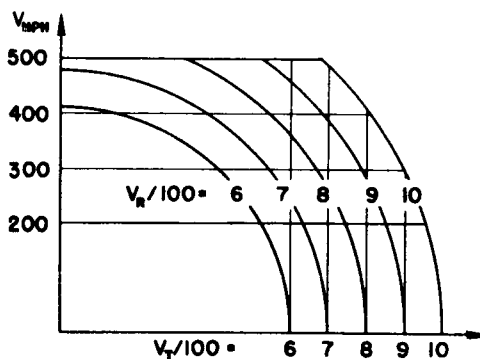
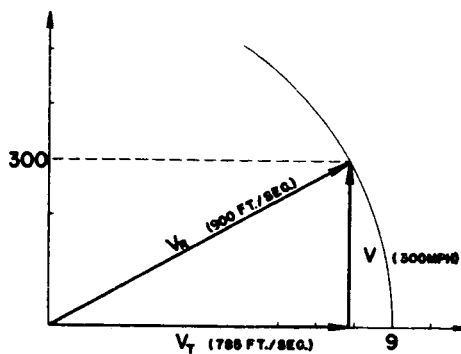


Figure 29.- Chart for evaluation of  $V_T$ .

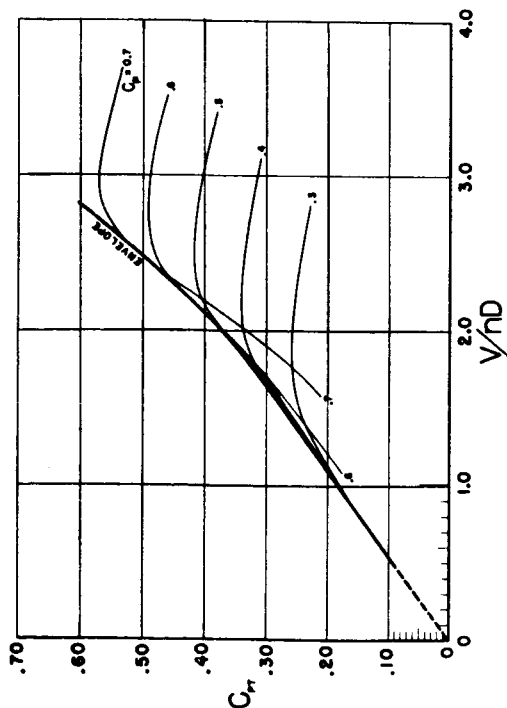
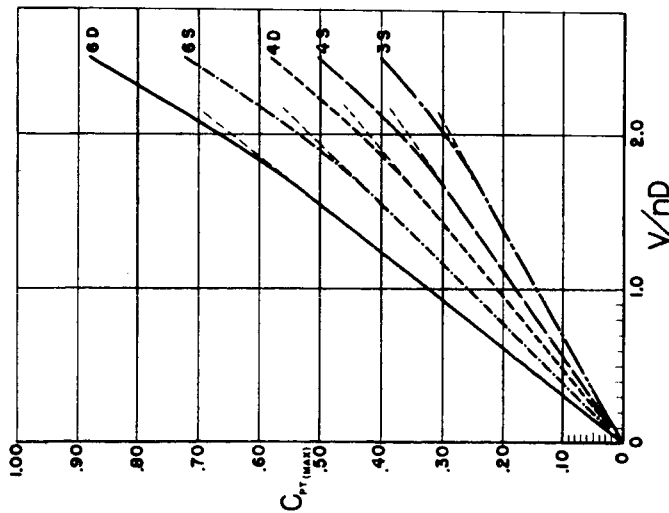


Figure 26.- Curves of figure 20 replotted to Cartesian coordinates.

Figure 27.- Envelopes of  $C_{pr}$  vs.  $V/nd$  for constant speed propellers with E-type blades and small spinners.



NACA

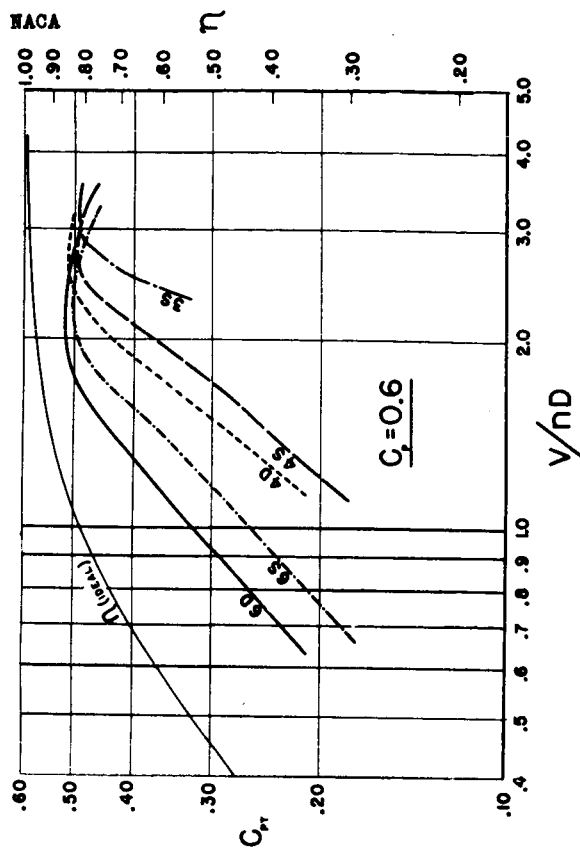


Figure 30.- Comparison of constant-speed propellers with E-type blades and small spinners at  $C_p=0.3$ .

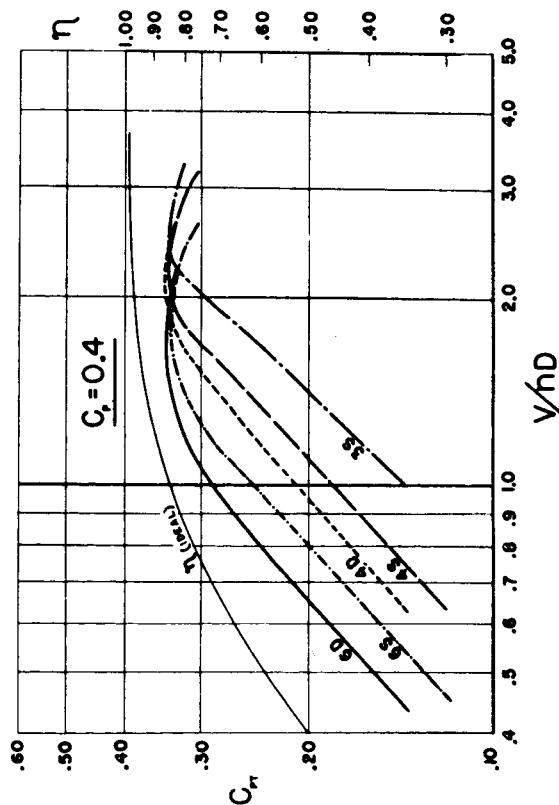


Figure 31.- Comparison of constant-speed propellers at  $C_p=0.4$ .

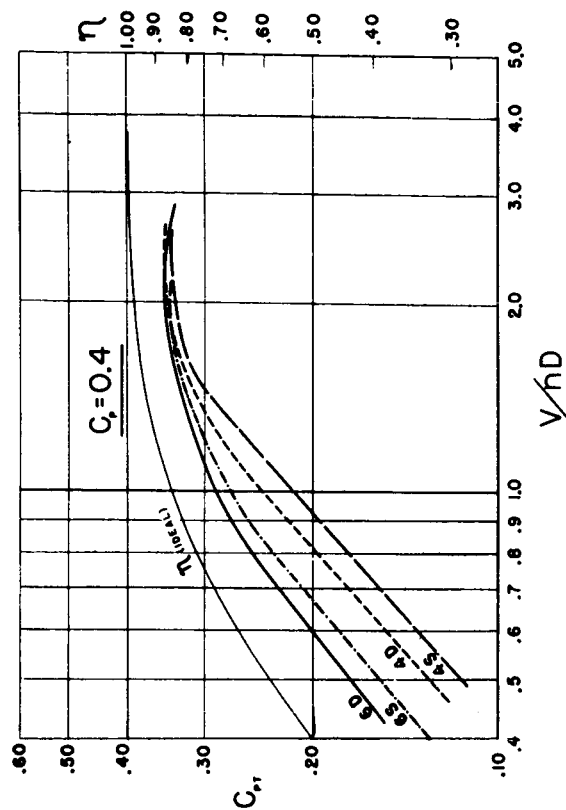


Figure 32.- Comparison of constant-speed propellers at  $C_p=0.6$ .

Figs. 30,31,32,33

Figure 33.- Full scale results corresponding to figure 31.

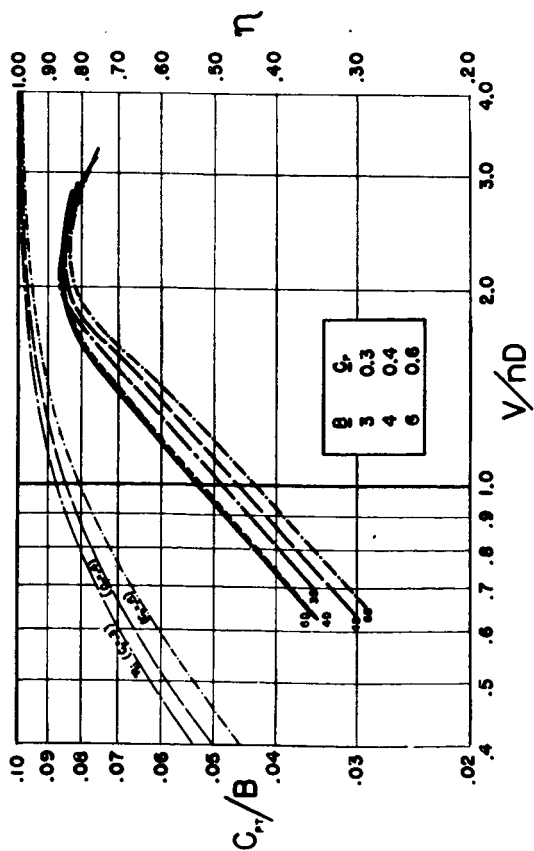


Figure 34.— Comparison of constant-speed propellers at equal blade loadings.

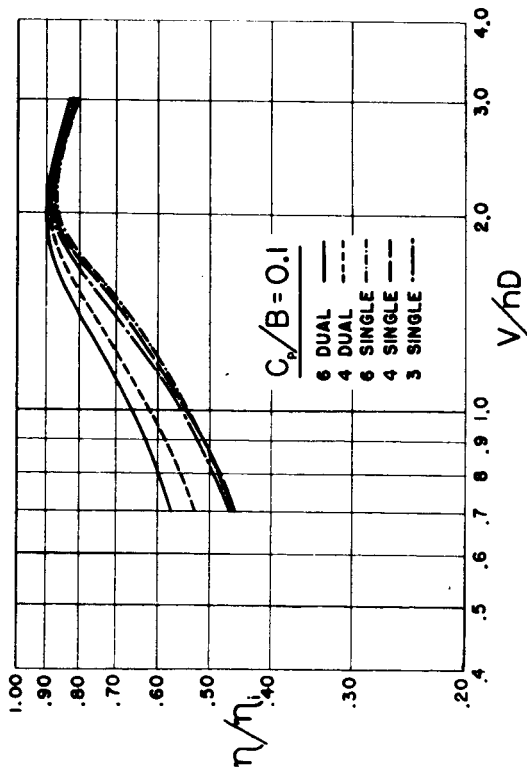


Figure 35.— Relative efficiencies for constant-speed propellers of equal blade loadings.

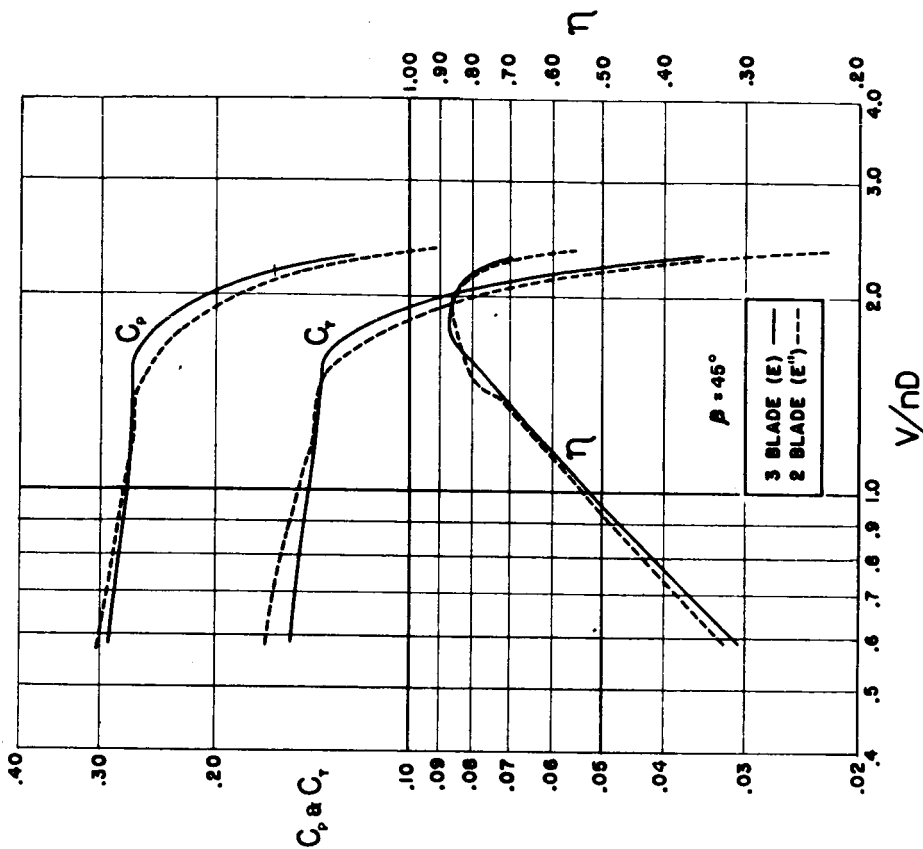


Figure 36.— Effects of number of blades at fixed solidity.

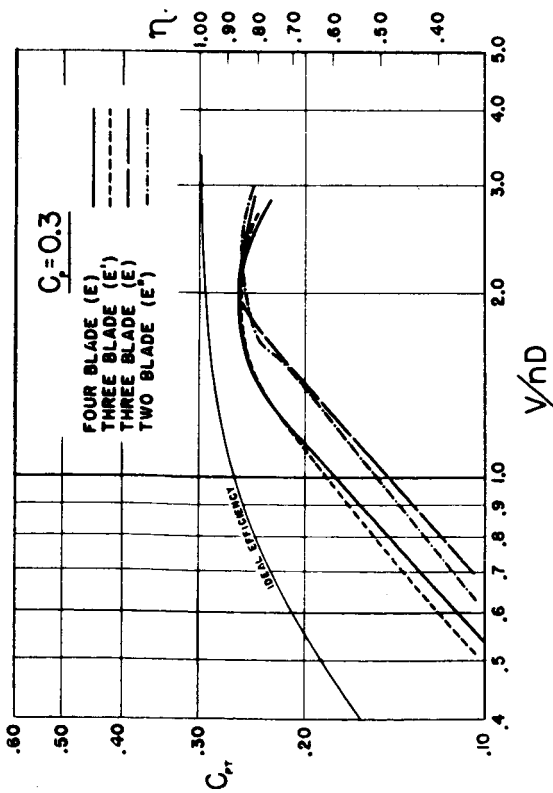


Figure 37.- Effects of number of blades on performance of constant-speed propellers at  $C_p = 0.3$ .

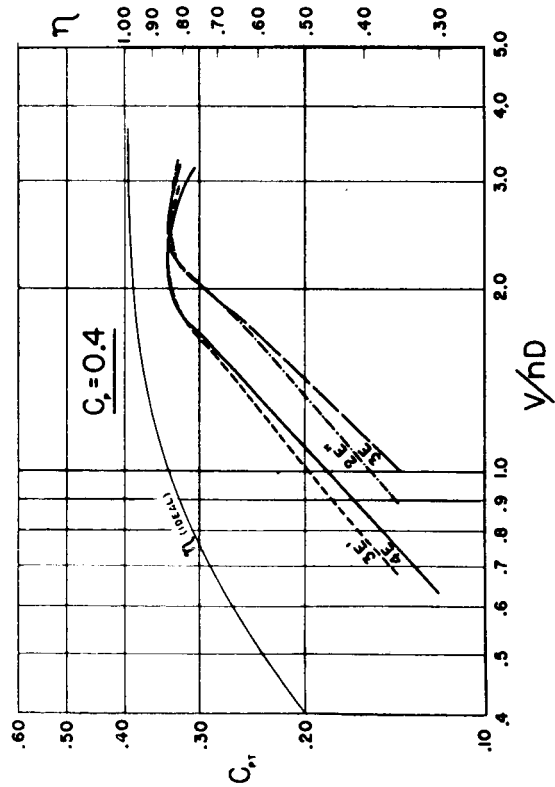


Figure 38.- Effects of number of blades on performance of constant-speed propellers at  $C_p = 0.4$ .

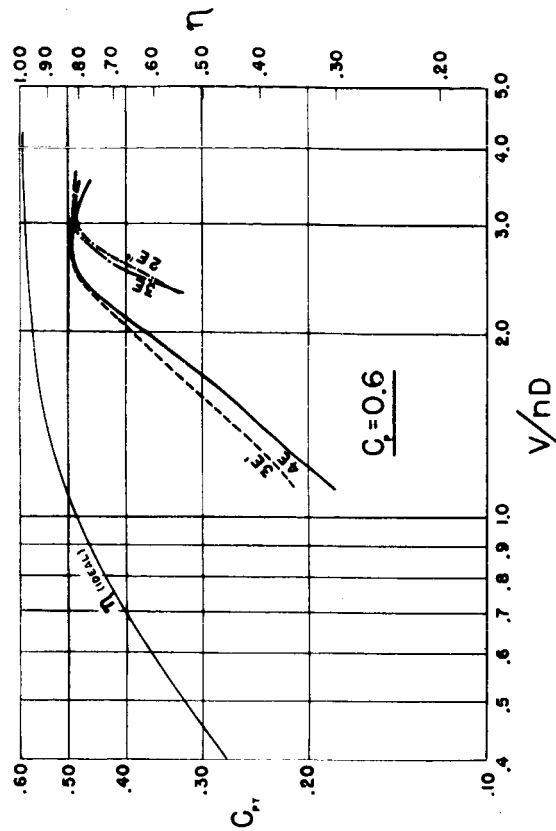


Figure 39.- Effects of number of blades on performance of constant-speed propellers at  $C_p = 0.6$ .